



ACADEMIC  
PRESS

Available online at [www.sciencedirect.com](http://www.sciencedirect.com)

SCIENCE @ DIRECT®

Appl. Comput. Harmon. Anal. 15 (2003) 33–69

---

---

Applied and  
Computational  
Harmonic Analysis

---

---

[www.elsevier.com/locate/acha](http://www.elsevier.com/locate/acha)

## 3D Fourier based discrete Radon transform

Amir Averbuch and Yoel Shkolnisky

*School of Computer Science, Tel Aviv University, Tel Aviv 69978, Israel*

Received 21 March 2002; accepted 22 October 2002

Communicated by Vladimir Rokhlin

---

### Abstract

The Radon transform is a fundamental tool in many areas. For example, in reconstruction of an image from its projections (CT scanning). Recently A. Averbuch et al. [SIAM J. Sci. Comput., submitted for publication] developed a coherent discrete definition of the 2D discrete Radon transform for 2D discrete images. The definition in [SIAM J. Sci. Comput., submitted for publication] is shown to be algebraically exact, invertible, and rapidly computable. We define a notion of 3D Radon transform for discrete 3D images (volumes) which is based on summation over planes with absolute slopes less than 1 in each direction. Values at nongrid locations are defined using trigonometric interpolation on a zero-padded grid. The 3D discrete definition of the Radon transform is shown to be geometrically faithful as the planes used for summation exhibit no wraparound effects. There exists a special set of planes in the 3D case for which the transform is rapidly computable and invertible. We describe an algorithm that computes the 3D discrete Radon transform which uses  $O(N \log N)$  operations, where  $N = n^3$  is the number of pixels in the image. The algorithm relies on the 3D discrete slice theorem that associates the Radon transform with the pseudo-polar Fourier transform. The pseudo-polar Fourier transform evaluates the Fourier transform on a non-Cartesian pointset, which we call the pseudo-polar grid. The rapid exact evaluation of the Fourier transform at these non-Cartesian grid points is possible using the fractional Fourier transform.

© 2003 Elsevier Inc. All rights reserved.

---

### 1. Introduction

An important problem in image processing is to reconstruct a cross-section of an object from several images of its projections. A projection is a shadowgram obtained by illuminating an object by penetrating radiation. Figure 1 shows a typical method for obtaining projections. Each horizontal line shown in this figure is a one-dimensional projection of a horizontal slice of the object. Each pixel of the projected image represents the total absorption of the X-ray along its path from the source to the detector. By rotating the source-detector assembly around the object, projections for several different angles can be obtained. The goal of *image reconstruction from projections* is to obtain an image of a cross-section of the object

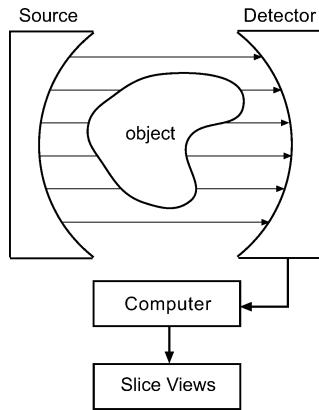


Fig. 1. An X-ray CT scanning system.

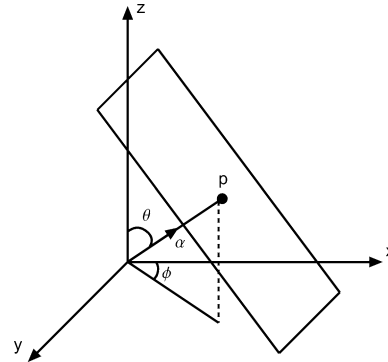


Fig. 2. 3D projection geometry.

from these projections. Imaging systems that generate such slice views are called CT (computerized tomography) scanners.

The Radon transform is the underlying fundamental concept [4,5] used for CT scanning, as well for a wide range of other disciplines, including radar imaging, geophysical imaging, nondestructive testing and medical imaging [3,8].

### 1.1. 3D continuous Radon transform

The 3D Radon transform is defined using 1D projections of a 3D object  $f(x, y, z)$  where these projections are obtained by integrating  $f(x, y, z)$  on a plane, whose orientation can be described by a unit vector  $\vec{\alpha}$  (see Fig. 2). Geometrically, the continuous 3D Radon transform maps a function in  $\mathbb{R}^3$  into the set of its plane integrals in  $\mathbb{R}^3$  (see Fig. 3). Formally, we have

**Definition 1.1** (3D continuous Radon transform). Given a 3D function  $f(\vec{x}) \triangleq f(x, y, z)$  and a plane (whose representation is given using the normal  $\vec{\alpha}$  and the distance  $s$  of the plane from the origin), the 3D continuous Radon transform of  $f$  for this plane is defined by

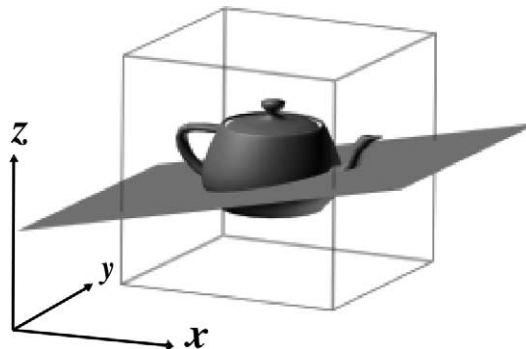


Fig. 3. 3D Radon transform illustration.

$$\begin{aligned} \mathfrak{R} f(\vec{\alpha}, s) &= \int_{-\infty}^{\infty} \int_{-\infty}^{\infty} \int_{-\infty}^{\infty} f(\vec{x}) \delta(\vec{x}^T \vec{\alpha} - s) d\vec{x} \\ &= \int_{-\infty}^{\infty} \int_{-\infty}^{\infty} \int_{-\infty}^{\infty} f(x, y, z) \delta(x \sin \theta \cos \phi + y \sin \theta \sin \phi + z \cos \theta - s) dx dy dz, \end{aligned} \quad (1.1)$$

where  $\vec{x} = [x, y, z]^T$ ,  $\vec{\alpha} = [\sin \theta \cos \phi, \sin \theta \sin \phi, \cos \theta]^T$ , and  $\delta$  is Dirac's delta function defined by

$$\delta(x) = 0, \quad x \neq 0, \quad \int_{-\infty}^{\infty} \delta(x) dx = 1. \quad (1.2)$$

The Radon transform maps the spatial domain  $(x, y, z)$  to the domain  $(\vec{\alpha}, s)$ . Each point in the  $(\vec{\alpha}, s)$  space corresponds to a plane in the spatial domain  $(x, y, z)$ . Note that  $(\vec{\alpha}, s)$  are not the polar coordinates of  $(x, y, z)$ .

The 3D continuous Radon transform satisfies the *3D Fourier slice theorem*, which states that the central slice  $\hat{f}(\xi \vec{\alpha})$  in the direction  $\vec{\alpha}$  of the 3D Fourier transform of  $f(\vec{x})$  equals  $\widehat{\mathfrak{R} f}(\vec{\alpha}, \xi)$ , that is

$$\widehat{\mathfrak{R} f}(\vec{\alpha}, \xi) = \hat{f}(\xi \vec{\alpha}) = \hat{f}(\xi \sin \theta \cos \phi, \xi \sin \theta \sin \phi, \xi \cos \theta), \quad (1.3)$$

where

$$\hat{f}(\xi_1, \xi_2, \xi_3) = \int_{-\infty}^{\infty} \int_{-\infty}^{\infty} \int_{-\infty}^{\infty} f(\vec{x}) e^{-2\pi i (\vec{x}^T \vec{\xi})} d\vec{x}, \quad \vec{\xi} = [\xi_1, \xi_2, \xi_3]^T, \quad \vec{x} = [x, y, z]^T \quad (1.4)$$

is the 3D Fourier transform of  $f$  and

$$\widehat{\mathfrak{R} f}(\vec{\alpha}, \xi) = \int_{-\infty}^{\infty} \mathfrak{R} f(\vec{\alpha}, s) e^{-2\pi i \xi s} ds \quad (1.5)$$

is 1D Fourier transform of the 3D Radon transform  $\mathfrak{R} f(\vec{\alpha}, s)$  along the parameter  $s$ .

### 1.2. Discretization of the Radon transform

For modern applications it is important to have a discrete analogues of  $\mathfrak{R} f$  for 3D digital images  $I = (I(u, v, w): -n/2 \leq u, v, w < n/2)$ .

The definition of the 3D discrete Radon transform should follow guidelines that were employed in [1,2] for the definition of the 2D discrete Radon transform. Specifically, any definition of the 3D discrete Radon transform should satisfy the following properties:

- (P1) *Algebraic exactness.* The transform should be based on a clear and rigorous definition, not, for example, on analogy to Eq. (1.1), e.g., formulations such as ‘we approximate the integral in Eq. (1.1) by a sum’.
- (P2) *Geometric fidelity.* The transform should be based on true geometric planes rather than planes which wrap around or are otherwise nongeometric.

- (P3) *Speed*. The transform should be rapidly computable, for example, admit an  $O(N \log N)$  algorithm where  $N = n^3$  is the size of the data in  $I$ .
- (P4) *Invertibility*. The transform should be invertible on its range. Moreover, there should be a fast reconstruction algorithm.
- (P5) *Parallels with continuum theory*. The transform should obey relations which parallel with those of the continuum theory (for example, relations with the Fourier transform).

In this paper, the approach suggested by [1] is generalized to prove that requirements (P1)–(P5) hold for the 3D case. This is accompanied by a complete analysis and proofs of the 3D case. Note that we only show invertibility (P4) for the 3D case. A reconstruction algorithm, however, is will be treated in another paper.

The organization of the paper is as follows. Section 1 gives an overview of the 3D continuous Radon transform and the discretization guidelines. Section 2 defines the 3D discrete Radon transform. It explains the selection of the transform parameters and details the geometry of the discrete definition. In Section 3 we prove the Fourier slice theorem for the 3D discrete Radon transform. In Section 4 we define the pseudo-polar grid and the pseudo-polar Fourier transform. In Section 5 we derive a fast algorithm for the computation of the 3D discrete Radon transform. Finally, in Section 6 we show that our notion of the 3D discrete Radon transform is invertible.

## 2. Definition of the 3D discrete Radon transform

Inspired by the definition of the 2D discrete Radon transform given in [1,2], the 3D discrete Radon transform is defined by summing the interpolated samples of a discrete array  $I(u, v, w)$  lying on planes which satisfy certain constraints. Formally, given a plane whose explicit equation is

$$z = s_1x + s_2y + t \quad (2.1)$$

(where the constraints on  $s_1$ ,  $s_2$ , and  $t$  will be determined shortly), we define the operator  $R_3I$  for the plane given in Eq. (2.1) by

$$R_3I(s_1, s_2, t) = \sum_{u=-n/2}^{n/2-1} \sum_{v=-n/2}^{n/2-1} \tilde{I}^3(u, v, s_1u + s_2v + t), \quad (2.2)$$

where

$$\tilde{I}^3(u, v, z) = \sum_{w=-n/2}^{n/2-1} I(u, v, w) D_m(z - w), \quad u, v = -\frac{n}{2}, \dots, \frac{n}{2} - 1, \quad z \in \mathbb{R}, \quad (2.3)$$

and  $D_m$  is the Dirichlet kernel given by

$$D_m(t) = \frac{\sin(\pi t)}{m \sin(\pi t/m)}, \quad m = 3n + 1. \quad (2.4)$$

The choice  $m = 3n + 1$  for the length of the Dirichlet kernel in Eq. (2.4) is critical and will be explained later.

We used the notation  $\tilde{I}^3$ , since we interpolate in the  $z$ -direction, which we consider the third direction. We refer to the  $x$ -,  $y$ -,  $z$ -direction, as the first, second, and third direction, respectively.

### 2.1. Selection of the parameters $t$ and $m$

In order for our definition to be geometrically faithful, the summation over planes must not wraparound over true samples of  $I$ . We want to sum only over “straight” planes. This can be achieved, as in the 2D case detailed in [1,2], by limiting the value  $z$  (of a plane  $z = s_1x + s_2y + t$ ) can have on the given domain (the image  $I$ ), limiting the slopes  $s_1, s_2$  and using padding to size  $m = 3n + 1$ . The size of  $m$  will be explained later. Limiting the value of the slopes  $s_1$  and  $s_2$  limits the value of  $z$  since  $x, y$  in Eq. (2.1) are bounded on the domain  $I$ .

Interpolated summation over planes do wraparound due to the periodic nature of the interpolation kernel  $D_m$ . If we pad, it wraps around over the zeros of the padding and not over true samples from  $I$ , and, therefore, we can think of it as if the wraparound never occurred (it lacks geometrical impact).

We start by limiting  $s_1$  and  $s_2$  to determine the size of  $m$  that is needed for padding. Using the interpolation kernel  $D_m$  is equivalent to symmetrically zero padding a given vector of samples to length  $m$  and then using trigonometric interpolation.

By taking a plane of the form  $z = s_1x + s_2y + t$  and by choosing  $|s_1| \leq 1$  and  $|s_2| \leq 1$ , we limit the  $z$  value of the plane over the domain  $-n/2 \leq x < n/2, -n/2 \leq y < n/2$ . Geometrically, we allow slopes of up to  $45^\circ$  in each direction ( $x$  and  $y$  directions). This is a reasonable restriction, while considering the symmetry of  $x, y$ , and  $z$ .

Fixing the ranges of  $s_1$  and  $s_2$ , we first determine the set of discrete intercepts  $t$  in Eq. (2.1), which is relevant to our choices of  $s_1$  and  $s_2$ . The geometrical interpretation of the intercept  $t$  for the plane  $z = s_1x + s_2y + t$  is the  $z$  value at  $x = 0, y = 0$  which measures the “intercept” of the plane at the origin.

We would like that for each family of planes, which corresponds to fixed  $s_1, s_2$ , and variable intercept  $t$ , to include at least all the planes in the given direction  $s_1, s_2$  that intersect with  $I(u, v, w)$ . The reason is that we want to sum over all planes in a given direction (fixed  $s_1, s_2$ ) that produce nontrivial projections of  $I$ , i.e., intersect the image  $I$ . Thus, for a given direction we must find at least all intercepts  $t$  that cause the plane  $z = s_1x + s_2y + t$  to intersect  $I$ .

It is easy to see that the extremal values of  $t$  are obtained on the boundary of the domain of  $s_1$  and  $s_2$ , i.e., for  $|s_1| = |s_2| = 1$ . The general plane equation reduces to  $z = x + y + t$  for  $s_1 = 1$  and  $s_2 = 1$ . Since we are interested only in  $z$  values that cause the plane to intersect  $I$ , we require that  $-n/2 \leq z < n/2$ . It follows that we first look for the maximal  $t$  such that

$$x + y + t < \frac{n}{2}$$

for at least one point from  $I$  (one point from the domain of  $x$  and  $y$ ). It is easy to see that the largest value of  $t$ , for which the plane  $z = x + y + t$  still satisfies  $z = x + y + t < n/2$  on  $I$ , is

$$t < \frac{3n}{2}.$$

For such a value of  $t$ , the extremal value of  $z$  in  $I$  is obtained for

$$x = -\frac{n}{2}, \quad y = -\frac{n}{2}$$

and in this case

$$z = x + y + t = -\frac{n}{2} - \frac{n}{2} + \frac{3n}{2} - 1 = \frac{n}{2} - 1.$$

For any larger  $t$ , there is no pair  $(x, y)$  in  $I$  such that the corresponding  $z$  satisfies  $z < n/2$ . Similarly, we want  $z$  to satisfy  $z \geq -n/2$  for at least one point from  $I$ . Again, it follows that the extremal plane in this case must satisfy  $x + y + t \geq -n/2$  for  $x < n/2$  and  $y < n/2$  and therefore

$$t \geq -\frac{3n}{2}.$$

We conclude that the relevant range of intercepts for the definition of the 3D discrete Radon transform must include the interval  $-3n/2 \leq t < 3n/2$ .

For the definition of the 3D discrete Radon transform we need the interval  $t$  to be of odd length. Therefore, we define  $t$  to be in the interval

$$-\frac{3n}{2} \leq t \leq \frac{3n}{2}.$$

Next, we must properly select the padding value  $m$  to retain geometric fidelity. We begin by checking the maximal  $z$  that the extremal plane can have (the plane that achieves the maximal  $z$  for the given domain). This value is achieved for  $s_1 = 1$  and  $s_2 = 1$ . Since  $t \leq 3n/2$ ,  $x < n/2$ ,  $y < n/2$ , it satisfies

$$z = s_1x + s_2y + t < \frac{n}{2} + \frac{n}{2} + \frac{3n}{2} = \frac{5n}{2}.$$

Suppose we use padding of size  $n + 1$  on top of  $I$  and  $n$  at the bottom of  $I$  along the  $z$ -axis. This looks as a box of  $(n/2) \times (n/2) \times (n + 1)$  zeros on top of  $I$  and  $(n/2) \times (n/2) \times n$  at the bottom of  $I$  along the  $z$ -axis (see Fig. 4 for 2D projections of  $I$  and its padding and Fig. 5 for a 3D illustration). In this case the extremal sample on the extremal plane will have  $z$  less than  $5n/2$ , or by taking the wraparound into account, less than  $-n/2$ , which is the first true sample of  $I$ . Hence, padding with boxes of zeros of total of size  $2n + 1$  eliminates wraparound of planes onto samples of  $I$ , and therefore the summation over these planes is a summation over geometric planes and not over planes which wraparound over true samples of  $I$ .

We conclude that to eliminate wraparound due to trigonometric interpolation, the padding size that is needed in the 3D case is  $2n + 1$  along the  $z$ -axis, meaning that the trigonometric interpolation takes place over  $3n + 1$  samples. In other words,  $m = 3n + 1$ , where  $m$  is the length of the interpolation kernel  $D_m$ .

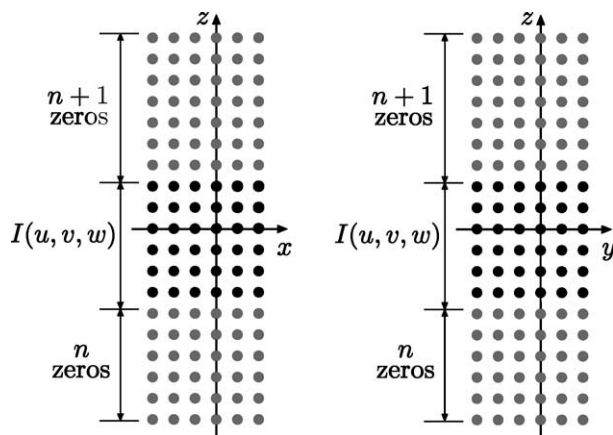


Fig. 4. Projections of a padded 3D image.

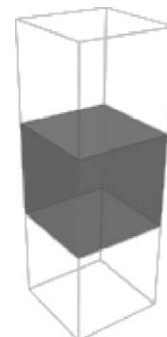


Fig. 5. A padded 3D image.

An important observation is that although we considered only planes of the form  $z = s_1x + s_2y + t$ , if we consider planes of the forms  $y = s_1x + s_2z + t$  and  $x = s_1y + s_2z + t$  with the same constraints  $|s_1| \leq 1$  and  $|s_2| \leq 1$ , we impose the same constraints on  $t$  and  $m$ , i.e.,  $-3n/2 \leq t \leq 3n/2$  and  $m = 3n + 1$ .

## 2.2. 3D geometry

The last observation leads to a definition of three types of planes, namely “ $x$ -planes”, “ $y$ -planes”, and “ $z$ -planes”.

### Definition 2.1.

- A plane of the form

$$x = s_1y + s_2z + t, \quad \text{where } |s_1| \leq 1, |s_2| \leq 1$$

is called  $x$ -plane.

- A plane of the form

$$y = s_1x + s_2z + t, \quad \text{where } |s_1| \leq 1, |s_2| \leq 1$$

is called  $y$ -plane.

- A plane of the form

$$z = s_1x + s_2y + t, \quad \text{where } |s_1| \leq 1, |s_2| \leq 1$$

is called  $z$ -plane.

**Lemma 2.1.** Each plane  $p$  in  $\mathbb{R}^3$  can be expressed as one of the plane types from Definition 2.1 ( $x$ -plane,  $y$ -plane, or  $z$ -plane).

**Proof.** Assume we take an arbitrary plane  $p$  in  $\mathbb{R}^3$

$$p: \alpha x + \beta y + \gamma z = t.$$

If two of the coefficients  $\alpha$ ,  $\beta$ , and  $\gamma$  are zero, the plane has one of the following forms:

- $x = t/\alpha$  ( $\beta = \gamma = 0$ ,  $\alpha \neq 0$ ), and it follows that the plane  $p$  is  $x$ -plane;
- $y = t/\beta$  ( $\alpha = \gamma = 0$ ,  $\beta \neq 0$ ), and it follows that the plane  $p$  is  $y$ -plane;
- $z = t/\gamma$  ( $\alpha = \beta = 0$ ,  $\gamma \neq 0$ ), and it follows that the plane  $p$  is  $z$ -plane.

Suppose that only one coefficient is zero, for example,  $\gamma = 0$ . One of two cases must hold

- If  $|\alpha| \geq |\beta|$  then the plane  $p$  is converted into

$$x = \left(-\frac{\beta}{\alpha}\right)y + \frac{t}{\alpha}$$

with  $|\beta/\alpha| \leq 1$ , and it follows that the plane is  $x$ -plane.

- If  $|\alpha| \leq |\beta|$  then the plane  $p$  is converted into

$$y = \left(-\frac{\alpha}{\beta}\right)x + \frac{t}{\beta}$$

with  $|\alpha/\beta| \leq 1$ , and it follows that the plane is  $y$ -plane.

Similar results hold if  $\alpha = 0$  or  $\beta = 0$ .

Remains to check the case where  $\alpha \neq 0$ ,  $\beta \neq 0$ ,  $\gamma \neq 0$ . Rewrite the plane equation

$$\alpha x + \beta y + \gamma z = t$$

as

$$z = \alpha' x + \beta' y + t'. \quad (2.5)$$

If  $|\alpha'| \leq 1$  and  $|\beta'| \leq 1$  then  $p$  is  $z$ -plane. Otherwise, one of the following must hold:

- If  $|\alpha'| \geq |\beta'|$  then  $|\alpha'| \geq 1$ . Rewrite Eq. (2.5) as

$$x = \left(-\frac{\beta'}{\alpha'}\right)y + \left(\frac{1}{\alpha'}\right)z - \frac{t'}{\alpha'}$$

with  $|1/\alpha'| \leq 1$ ,  $|\beta'/\alpha'| \leq 1$ , and it follows that  $p$  is  $x$ -plane.

- If  $|\alpha'| \leq |\beta'|$  then  $|\beta'| \geq 1$ . Rewrite Eq. (2.5) as

$$y = \left(-\frac{\alpha'}{\beta'}\right)x + \left(\frac{1}{\beta'}\right)z - \frac{t'}{\beta'}$$

with  $|\alpha'/\beta'| \leq 1$ ,  $|1/\beta'| \leq 1$ , and it follows that  $p$  is  $y$ -plane.

We conclude that every plane  $p$  can be written as either  $x$ -plane,  $y$ -plane, or  $z$ -plane.  $\square$

### 2.3. Formal definition of the 3D Radon transform

We first define the 3D Radon transform on discrete 3D images  $I$ , and on continuous set of planes, and later we discretize the planes set.

We define three summation operators, one for each type of plane ( $x$ -plane,  $y$ -plane,  $z$ -plane defined in Definition 2.1). Each summation operator takes a plane and an image  $I$  and calculates the sum of the samples from  $I$  “on” the plane. More precisely, it calculates the sum of the interpolated samples of  $I$  on the plane.

**Definition 2.2** (*Summation operators*). Let  $I$  be a discrete image of size  $n \times n \times n$ .

- For  $x$ -plane we define

$$\text{Radon}(\{x = s_1 y + s_2 z + t\}, I) = \sum_{v=-n/2}^{n/2-1} \sum_{w=-n/2}^{n/2-1} \tilde{I}^1(s_1 v + s_2 w + t, v, w), \quad (2.6)$$

where

$$\tilde{I}^1(x, v, w) = \sum_{u=-n/2}^{n/2-1} I(u, v, w) D_m(x - u), \quad v, w \in \left\{-\frac{n}{2}, \dots, \frac{n}{2} - 1\right\}, \quad x \in \mathbb{R}. \quad (2.7)$$

- For  $y$ -plane we define

$$\text{Radon}(\{y = s_1x + s_2z + t\}, I) = \sum_{u=-n/2}^{n/2-1} \sum_{w=-n/2}^{n/2-1} \tilde{I}^2(u, s_1u + s_2w + t, w), \quad (2.8)$$

where

$$\tilde{I}^2(u, y, w) = \sum_{v=-n/2}^{n/2-1} I(u, v, w) D_m(y - v), \quad u, w \in \left\{ -\frac{n}{2}, \dots, \frac{n}{2} - 1 \right\}, y \in \mathbb{R}. \quad (2.9)$$

- For  $z$ -plane we define

$$\text{Radon}(\{z = s_1x + s_2y + t\}, I) = \sum_{u=-n/2}^{n/2-1} \sum_{v=-n/2}^{n/2-1} \tilde{I}^3(u, v, s_1u + s_2v + t), \quad (2.10)$$

where

$$\tilde{I}^3(u, v, z) = \sum_{w=-n/2}^{n/2-1} I(u, v, w) D_m(z - w), \quad u, v \in \left\{ -\frac{n}{2}, \dots, \frac{n}{2} - 1 \right\}, z \in \mathbb{R}. \quad (2.11)$$

Using the summation operators (Eqs. (2.6), (2.8), and (2.10)), we define three Radon operators  $R_i I$  ( $i = 1, 2, 3$ ) for a 3D image (volume)  $I$  as

- For  $x$ -plane  $x = s_1y + s_2z + t$  define

$$R_1 I(s_1, s_2, t) \triangleq \text{Radon}(x = s_1y + s_2z + t, I). \quad (2.12)$$

- For  $y$ -plane  $y = s_1x + s_2z + t$  define

$$R_2 I(s_1, s_2, t) \triangleq \text{Radon}(y = s_1x + s_2z + t, I). \quad (2.13)$$

- For  $z$ -plane  $z = s_1x + s_2y + t$  define

$$R_3 I(s_1, s_2, t) \triangleq \text{Radon}(z = s_1x + s_2y + t, I). \quad (2.14)$$

For a given plane  $p$  we can classify it by Lemma 2.1 as an either  $x$ -plane,  $y$ -plane, or  $z$ -plane with slopes  $s_1$  and  $s_2$ . We define the “canonization transform” that takes an arbitrary plane  $p$  and transforms it into one of the plane types that were defined in Definition 2.1.

**Definition 2.3** (*Canonization transform*). Given a plane  $p$  whose equation is given by

$$p: \alpha x + \beta y + \gamma z + t = 0,$$

we denote by  $P$  the set of all planes  $p$  in  $\mathbb{R}^3$ . Let  $C : P \rightarrow \mathbb{R}^4$  be the transformation that takes a plane  $p \in P$  and transforms it into one of the plane types:  $x$ -plane,  $y$ -plane, or  $z$ -plane. For  $p \in P$

$$C(p) \triangleq (q, s_1, s_2, t'),$$

where

- $q = 1$  if  $C(p)$  is  $x$ -plane  $x = s_1y + s_2z + t'$  with  $-1 \leq s_1, s_2 \leq 1$ ;
- $q = 2$  if  $C(p)$  is  $y$ -plane  $y = s_1x + s_2z + t'$  with  $-1 \leq s_1, s_2 \leq 1$ ;
- $q = 3$  if  $C(p)$  is  $z$ -plane  $z = s_1x + s_2y + t'$  with  $-1 \leq s_1, s_2 \leq 1$ .

**Definition 2.4** (3D Radon transform). Assume that  $I$  is a discrete image of size  $n \times n \times n$  and the plane  $p$  is determined by  $C(p)$  from Definition 2.3. Then, the 3D Radon transform of  $I$  on  $p$  is defined by

$$RI(p, I) = RI(s_1, s_2, t) \triangleq \begin{cases} R_1I(s_1, s_2, t), & q = 1, \\ R_2I(s_1, s_2, t), & q = 2, \\ R_3I(s_1, s_2, t), & q = 3, \end{cases} \quad (2.15)$$

where  $R_1, R_2,$  and  $R_3$  were defined in Eqs. (2.12)–(2.14) and  $q, s_1, s_2,$  and  $t$  are determined from  $C(p)$  according to Definition 2.3.

#### 2.4. Traditional $(\phi, \theta)$ representation of planes

The definition of the 3D Radon transform uses slopes and intercepts to designate a specific plane. The notation of a plane using slopes is less common and should be further explained. Usually, a plane in  $\mathbb{R}^3$  is defined using a unit normal vector  $\vec{n}$  and the distance of the plane from the origin. Formally,  $\langle \vec{n}, (x, y, z) \rangle = t$ , where  $\vec{n}$  can be represented using the angles  $(\phi, \theta)$  (see Fig. 2) as

$$\vec{n} = (\cos \phi \sin \theta, \sin \phi \sin \theta, \cos \theta).$$

We would like to find a correlation between the  $(\phi, \theta, t)$  representation of a plane and the explicit plane representation (using slopes). We begin by inspecting the explicit equation of a  $z$ -plane  $z = s_1x + s_2y + t$  where  $|s_1| \leq 1$  and  $|s_2| \leq 1$ . This can be rewritten as

$$\langle (-s_1, -s_2, 1), (x, y, z) \rangle = t.$$

Define

$$s = \|(-s_1, -s_2, 1)\| = \sqrt{s_1^2 + s_2^2 + 1}$$

and by normalizing the normal vector, we obtain

$$\left\langle \left( -\frac{s_1}{s}, -\frac{s_2}{s}, \frac{1}{s} \right), (x, y, z) \right\rangle = \frac{t}{s},$$

where  $\vec{n} = (-s_1/s, -s_2/s, 1/s)$  is the unit normal vector to the plane.

By expressing  $(\phi, \theta)$  of the vector  $\vec{n}$  using  $s_1$  and  $s_2$  we obtain

$$\begin{cases} \tan \phi = \frac{-s_2/s}{-s_1/s} = \frac{s_2}{s_1}, \\ \tan \theta = \pm \frac{\sqrt{s_1^2/s^2 + s_2^2/s^2}}{1/s} = \pm \sqrt{s_1^2 + s_2^2}. \end{cases}$$

The range of  $(\phi, \theta)$ , which corresponds to  $z$ -planes, is

$$\tan \phi = \frac{s_2}{s_1}, \quad \tan \theta = \pm \sqrt{s_1^2 + s_2^2},$$

where  $|s_1| \leq 1$  and  $|s_2| \leq 1$ .

Resolving for  $s_1$  and  $s_2$ , we obtain

$$\begin{cases} s_1^2 = \frac{\tan^2 \theta}{1 + \tan^2 \phi}, \\ s_2^2 = \frac{\tan^2 \theta \tan^2 \phi}{1 + \tan^2 \phi}. \end{cases} \quad (2.16)$$

Since  $|s_1| \leq 1$  and  $|s_2| \leq 1$  it follows that:

$$\begin{cases} \frac{\tan^2 \theta}{1 + \tan^2 \phi} \leq 1, \\ \frac{\tan^2 \theta \tan^2 \phi}{1 + \tan^2 \phi} \leq 1. \end{cases} \quad (2.17)$$

We conclude that the range of  $(\phi, \theta)$ , which defines all  $z$ -planes, satisfies Eq. (2.17). Equation (2.17) does not define a domain that is simple to describe and therefore it is less convenient than the slopes notation used to define our notion of 3D Radon transform (Definition 2.4).

Inspecting the relations between  $x$ -planes and  $y$ -planes and the  $(\phi, \theta)$  notation yields similar results and will not be detailed here.

Equations (2.16) and (2.17) allow us to compute the 3D Radon transform for a plane whose normal is given as a pair of angles  $(\phi, \theta)$ , by using transformation to explicit plane representation with  $s_1$  and  $s_2$ .

### 3. 3D discrete Fourier slice theorem

Equation (1.3) states the well-known Fourier slice theorem for the 3D continuous Radon transform. This slice theorem defines the relation between the 3D continuous Radon transform  $\mathfrak{R}f$  of a function  $f(x, y, z)$  and the 3D Fourier transform of  $f$  along some radial line. Moreover, it allows us to evaluate the continuous Radon transform using the 3D Fourier transform of the function  $f$ .

Following the continuum theory, we will look for the relation between the discrete Radon transform and the 3D discrete Fourier transform of the image  $I$ . We use this relation to compute the discrete Radon transform. In order to derive such a relation we will develop an alternative definition for  $RI$  (Eq. (2.15)) which is more suited for such a construction.

We begin by defining some auxiliary operators (translation, extension, truncation, shearing, and backprojection operators) which will be used for the evaluation of the 1D Fourier transform of  $RI$ . The key-idea behind the alternative formulation of the 3D Radon transform (to be explained shortly) is that summation over the plane  $(u, v, s_1u + s_2v + t)$  in Eq. (2.10) is equivalent to a shift of the vector  $(u, v, \cdot)$  by  $-(s_1u + s_2v)$  (using trigonometric interpolation) and summation over the plane  $z = t$ .

Since we use trigonometric interpolation, which gives circular shift, it is necessary to use  $m = 3n + 1$  to avoid plane wraparound and achieve geometric fidelity (see Section 2.1).

**Definition 3.1** (*Translation operator*). Let

$$T_\tau : \mathbb{C}^m \rightarrow \mathbb{C}^m, \quad m = 3n + 1.$$

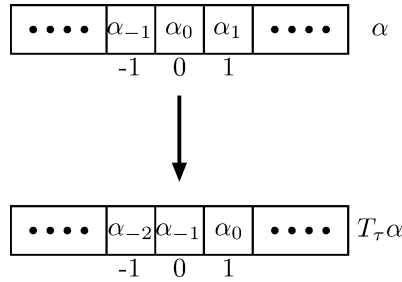


Fig. 6. Translation of the vector  $\alpha$  with  $\tau = 1$ .

Given a vector  $\alpha = (\alpha_t; -3n/2 \leq t \leq 3n/2)$  and some  $\tau \in \mathbb{R}$ , we define the vector  $T_\tau \alpha = ((T_\tau \alpha)_u) - 3n/2 \leq u \leq 3n/2$ , where

$$(T_\tau \alpha)_u = \sum_{i=-3n/2}^{3n/2} \alpha_i D_m(u - i - \tau), \quad m = 3n + 1 \tag{3.1}$$

and  $D_m$  defined in Eq. (2.4).

The operator  $T_\tau$  translates the vector  $\alpha$  by  $\tau$ , performing trigonometric interpolation when necessary. For example, assume  $\tau = 1$ . Calculating  $(T_\tau \alpha)_u$  for  $u = 0$  (the zero element of the translated vector) gives

$$(T_\tau \alpha)_0 = \sum_{i=-3n/2}^{3n/2} \alpha_i D_m(-i - 1).$$

Since  $D_m$  is zero on all integers except 0, the only nonzero element in the sum occurs at  $i = -1$  (for which  $D_m(0) = 1$ ).

Thus,  $(T_\tau \alpha)_0 = \alpha_{-1}$  and the operator  $T_1$  translated  $\alpha$  one place to the right (see Fig. 6).

**Definition 3.2 (Adjoint operator).** Let  $T$  be an operator  $T : X \rightarrow Y$ . The operator  $G : Y \rightarrow X$  is called the *adjoint* of  $T$ , denoted by  $G = \text{adj } T$ , if for each  $\alpha \in X$ ,  $\beta \in Y$   $\langle T\alpha, \beta \rangle = \langle \alpha, G\beta \rangle$ .

**Lemma 3.1.**  $\text{adj } T_\tau = T_{-\tau}$ .

**Proof.** Let  $\alpha, \beta \in \mathbb{C}^m$ ,  $m = 3n + 1$ .

$$\begin{aligned} \langle T_\tau \alpha, \beta \rangle &= \sum_{i=-3n/2}^{3n/2} (T_\tau \alpha)_i \beta_i^* = \sum_{i=-3n/2}^{3n/2} \left( \sum_{j=-3n/2}^{3n/2} \alpha_j D_m(i - j - \tau) \right) \beta_i^* \\ &= \sum_{i=-3n/2}^{3n/2} \left( \sum_{j=-3n/2}^{3n/2} \beta_i^* \alpha_j D_m(i - j - \tau) \right) = \sum_{j=-3n/2}^{3n/2} \left( \sum_{i=-3n/2}^{3n/2} \beta_i^* D_m(i - j - \tau) \right) \alpha_j \\ &= \sum_{j=-3n/2}^{3n/2} \left( \sum_{i=-3n/2}^{3n/2} \beta_i^* D_m(i - j - \tau) \right) \alpha_j = \sum_{j=-3n/2}^{3n/2} \left( \sum_{i=-3n/2}^{3n/2} \beta_i D_m(i - j - \tau) \right)^* \alpha_j \end{aligned}$$

$$\begin{aligned}
 &= \sum_{j=-3n/2}^{3n/2} \left( \sum_{i=-3n/2}^{3n/2} \beta_i D_m(j-i+\tau) \right)^* \alpha_j \quad (\text{since } D_m(t) = D_m(-t)) \\
 &= \sum_{j=-3n/2}^{3n/2} (T_{-\tau}\beta)_j^* \alpha_j = \langle \alpha, T_{-\tau}\beta \rangle.
 \end{aligned}$$

This yields

$$T_{-\tau} = \text{adj } T_{\tau}. \quad \square$$

An important property of the translation operator  $T_{\tau}$  is that the translation of an exponential is algebraically exact. In other words, the translation of a vector of samples of an exponential  $e^{2\pi i kx/m}$  is exactly the same as resampling the exponential in the translated points. This observation will have a great importance in proving the Fourier slice theorem.

**Lemma 3.2.** Let  $m = 3n + 1$ ,  $\varphi(x) = e^{2\pi i kx/m}$ . Define the vector  $\phi \in \mathbb{C}^m$  to be  $\phi_t = \varphi(t)$ ,  $-3n/2 \leq t \leq 3n/2$ . Then

$$(T_{\tau}\phi)_t = \varphi(t - \tau), \quad -\frac{3n}{2} \leq t \leq \frac{3n}{2},$$

where  $T_{\tau}$  defined in Eq. (3.1).

**Proof.** Given a vector  $\alpha = (\alpha_t: -3n/2 \leq t \leq 3n/2)$ , the interpolated underlying function, when using trigonometric interpolation is

$$I_m(x, \alpha) = \sum_{j=-3n/2}^{3n/2} \alpha_j D_m(x - j), \tag{3.2}$$

where  $D_m$  was defined in Eq. (2.4).  $I_m(x, \alpha)$  denotes interpolation of the vector  $\alpha$  at the point  $x$ . We note that from Eq. (3.1) we have

$$(T_{\tau}\alpha)_t = \sum_{j=-3n/2}^{3n/2} \alpha_j D_m(t - j - \tau) = I_m(t - \tau, \alpha) \tag{3.3}$$

meaning that translating the vector  $\alpha = (\alpha_t: -3n/2 \leq t \leq 3n/2)$  is simply resampling the interpolated function  $I_m(x, \alpha)$ . In our case we are looking at the vector  $\phi \in \mathbb{C}^m$ :  $\phi_t = \varphi(t)$ ,  $-3n/2 \leq t \leq 3n/2$ , of samples from the continuous function  $\varphi(x) = e^{2\pi i kx/m}$  and therefore Eq. (3.2) has the form

$$I_m(x, \phi) = \sum_{j=-3n/2}^{3n/2} \phi_j D_m(x - j). \tag{3.4}$$

We show that Eq. (3.4) can be rephrased as a trigonometric polynomial of the form

$$I_m(x, \phi) = \sum_{k=-3n/2}^{3n/2} \beta_k e^{2\pi i kx/m} \tag{3.5}$$

with some  $\beta_k$ . From Eq. (2.4)

$$D_m(t) = \frac{\sin(\pi t)}{m \sin(\pi t/m)}, \quad m = 3n + 1. \quad (3.6)$$

Rewriting Eq. (3.6) we have for  $m = 3n + 1$

$$D_m(t) = \frac{\sin(\pi t)}{m \sin(\pi t/m)} \quad (3.7)$$

$$= \frac{2 \sin(\pi t)}{m 2 \sin(\pi t/m)} \quad (3.8)$$

$$= \frac{2 \sin\left(\frac{3n+1}{2} \frac{2\pi t}{3n+1}\right)}{m 2 \sin\left(\frac{1}{2} \frac{2\pi t}{3n+1}\right)}. \quad (3.9)$$

We take the identity

$$\frac{1}{2} + \sum_{k=1}^L \cos(kx) = \frac{\sin((L+1/2)x)}{2 \sin(x/2)} \quad (3.10)$$

and by substituting  $L = 3n/2$  in Eq. (3.10) we obtain

$$\frac{1}{2} + \sum_{k=1}^{3n/2} \cos(kx) = \frac{\sin(((3n+1)/2)x)}{2 \sin(x/2)}. \quad (3.11)$$

By substituting  $x = (2\pi t)/(3n+1)$  into Eq. (3.11) we obtain

$$\frac{1}{2} + \sum_{k=1}^n \cos\left(k \frac{2\pi t}{3n+1}\right) = \frac{\sin\left(\frac{3n+1}{2} \frac{2\pi t}{3n+1}\right)}{2 \sin\left(\frac{1}{2} \frac{2\pi t}{3n+1}\right)}. \quad (3.12)$$

Using Eqs. (3.12) and (3.9) we have

$$D_m(t) = \frac{2}{m} \left( \frac{1}{2} + \sum_{k=1}^{3n/2} \cos\left(k \frac{2\pi t}{3n+1}\right) \right), \quad m = 3n + 1. \quad (3.13)$$

Since each term  $\cos(k(2\pi t)/(3n+1))$  in Eq. (3.13) can be written as

$$\cos\left(k \frac{2\pi t}{3n+1}\right) = \gamma_k e^{ik(2\pi t/m)} + \lambda_k e^{-ik(2\pi t/m)}, \quad m = 3n + 1 \quad (3.14)$$

for some  $\gamma_k$  and  $\lambda_k$ , then Eq. (3.13) can be written as

$$D_m(t) = \frac{2}{m} \left( \frac{1}{2} + \sum_{k=1}^{3n/2} (\gamma_k e^{ik(2\pi t/m)} + \lambda_k e^{-ik(2\pi t/m)}) \right) = \sum_{k=-3n/2}^{3n/2} \mu_k e^{ik(2\pi t/m)} \quad (3.15)$$

for some coefficients  $\mu_k$ . Therefore, using Eq. (3.15), Eq. (3.4) can be written as

$$I_m(x, \phi) = \sum_{j=-3n/2}^{3n/2} \phi_j D_m(x - j) \quad (3.16)$$

$$= \sum_{j=-3n/2}^{3n/2} \phi_j \sum_{k=-3n/2}^{3n/2} \mu_k e^{ik(2\pi(x-j)/m)} \tag{3.17}$$

$$= \sum_{j=-3n/2}^{3n/2} \phi_j \sum_{k=-3n/2}^{3n/2} \mu_k e^{-2\pi i k j / m} e^{ik(2\pi x / m)} \tag{3.18}$$

$$= \sum_{k=-3n/2}^{3n/2} \beta_k e^{2\pi i k x / m}, \tag{3.19}$$

where Eq. (3.19) follows since Eq. (3.18) is aggregation of terms of the form  $e^{2\pi i k x / m}$ .

Using Eq. (3.5) we have that  $\varphi(x) = e^{2\pi i k x / m}$  and  $I_m(x, \phi)$  are 2 trigonometric polynomials that coincide on  $3n + 1$  points  $t = -3n/2, \dots, 3n/2$ , and hence (see [6]), we have

$$\varphi(x) \equiv I_m(x, \phi).$$

Therefore, by Eq. (3.3)

$$\varphi(t - \tau) \equiv I_m(t - \tau, \phi) = (T_\tau \phi)_t. \quad \square$$

The 3D image space  $\mathbb{I}_{k \times l \times q}$  for  $k, l$ , and  $q$  even, is defined as

$$\mathbb{I}_{k \times l \times q} = \left\{ I(x, y, z) \in \mathbb{C} \left| \begin{array}{l} x \in \mathbb{Z}, -k/2 \leq x < k/2 \\ y \in \mathbb{Z}, -l/2 \leq y < l/2 \\ z \in \mathbb{Z}, -q/2 \leq z < q/2 \end{array} \right. \right\}. \tag{3.20}$$

If, for example,  $k = 2p + 1$ , then  $\mathbb{I}_{k \times l \times q}$  is defined as

$$\mathbb{I}_{k \times l \times q} = \left\{ I(x, y, z) \in \mathbb{C} \left| \begin{array}{l} x \in \mathbb{Z}, -p \leq x \leq p \\ y \in \mathbb{Z}, -l/2 \leq y < l/2 \\ z \in \mathbb{Z}, -q/2 \leq z < q/2 \end{array} \right. \right\}. \tag{3.21}$$

**Definition 3.3** (*Extension operators*).  $E^1, E^2$ , and  $E^3$

$$E^1 : \mathbb{I}_{n \times n \times n} \rightarrow \mathbb{I}_{m \times n \times n}, \quad E^2 : \mathbb{I}_{n \times n \times n} \rightarrow \mathbb{I}_{n \times m \times n}, \quad E^3 : \mathbb{I}_{n \times n \times n} \rightarrow \mathbb{I}_{n \times n \times m},$$

where  $m = 3n + 1$  and

$$E^i I(u, v, w) = \begin{cases} I(u, v, w), & -n/2 \leq u, v, w < n/2, \quad i = 1, 2, 3, \\ 0, & \text{otherwise} \end{cases} \tag{3.22}$$

are called the *extension operators*.

We pad with zeros the interpolated direction. For example, if we interpolate  $z$  for each  $(x, y)$  then we pad in the  $z$  direction.

We refer to  $I$  as a 3D function rather than a 3D array, meaning that for  $I(u, v, w)$ , the parameters  $(u, v, w)$  are referred to as the  $x, y, z$  coordinates, respectively.

Complementary to the *extension operators*  $E^i$  we define the *truncation operators*.

**Definition 3.4** (Truncation operators).  $U^1$ ,  $U^2$ , and  $U^3$

$$U^1: \mathbb{I}_{m \times n \times n} \rightarrow \mathbb{I}_{n \times n \times n}, \quad U^2: \mathbb{I}_{n \times m \times n} \rightarrow \mathbb{I}_{n \times n \times n}, \quad U^3: \mathbb{I}_{n \times n \times m} \rightarrow \mathbb{I}_{n \times n \times n},$$

where  $m = 3n + 1$  and

$$U^i I(u, v, w) = I(u, v, w), \quad -n/2 \leq u, v, w < n/2, \quad i = 1, 2, 3 \quad (3.23)$$

are called the *truncation operators*.

We have the following relation between  $E^i$  and  $U^i$  ( $i = 1, 2, 3$ ).

**Lemma 3.3.**  $\text{adj } E^i = U^i$ ,  $i = 1, 2, 3$ .

**Proof.** We will prove that  $\text{adj } E^3 = U^3$ . The proofs for  $E^1$  and  $E^2$  are identical.

Assume  $m = 3n + 1$ . Let  $A \in \mathbb{I}_{n \times n \times n}$ ,  $B \in \mathbb{I}_{n \times n \times m}$ .

$$\begin{aligned} \langle E^3 A, B \rangle &= \sum_{i=-n/2}^{n/2-1} \sum_{j=-n/2}^{n/2-1} \sum_{k=-3n/2}^{3n/2} (E^3 A)(i, j, k) B^*(i, j, k) \\ &= \sum_{i=-n/2}^{n/2-1} \sum_{j=-n/2}^{n/2-1} \sum_{k=-n/2}^{n/2-1} (E^3 A)(i, j, k) B^*(i, j, k) \end{aligned} \quad (3.24)$$

$$= \sum_{i=-n/2}^{n/2-1} \sum_{j=-n/2}^{n/2-1} \sum_{k=-n/2}^{n/2-1} A(i, j, k) B^*(i, j, k), \quad (3.25)$$

where Eq. (3.24) follows since  $E^3 A(i, j, k) = 0$  for  $k \geq n/2$  or  $k < -n/2$  (by Eq. (3.22)) and Eq. (3.25) follows since  $E^3 A(i, j, k) = A(i, j, k)$  for the indices  $-n/2 \leq i, j, k < n/2$ .

On the other hand, from the definition of  $U^1$  (Eq. (3.23)), we have

$$\begin{aligned} \langle A, U^3 B \rangle &= \sum_{i=-n/2}^{n/2-1} \sum_{j=-n/2}^{n/2-1} \sum_{k=-n/2}^{n/2-1} A(i, j, k) (U^3 B)^*(i, j, k) \\ &= \sum_{i=-n/2}^{n/2-1} \sum_{j=-n/2}^{n/2-1} \sum_{k=-n/2}^{n/2-1} A(i, j, k) B^*(i, j, k). \end{aligned}$$

Therefore,

$$\langle E^3 A, B \rangle = \langle A, U^3 B \rangle.$$

We get

$$U^3 = \text{adj } E^3. \quad \square$$

Consider a  $z$ -plane  $p$ , whose explicit equation is  $z = s_1 x + s_2 y + t$ . We shift  $z$  for each point  $(x, y)$  on the plane  $p$  by  $-(s_1 x + s_2 y)$ . This way the plane  $p$  is transformed into a plane of the form  $z = t$ . We denote this shift for  $z$ -plane by  $\tau^3(u, v, s_1, s_2)$ .

Similarly, we define the size of the shift at each point for each type of plane.

**Definition 3.5** (*Translation magnitude*). Let  $\tau^1$ ,  $\tau^2$ , and  $\tau^3$  be the “translation magnitude” of  $x$ -plane,  $y$ -plane, and  $z$ -plane, respectively. We define

For  $x$ -plane  $x = s_1y + s_2z + t$

$$\tau^1(s_1, s_2, v, w) = s_1v + s_2w. \tag{3.26}$$

For  $y$ -plane  $y = s_1x + s_2z + t$

$$\tau^2(s_1, s_2, u, w) = s_1u + s_2w. \tag{3.27}$$

For  $z$ -plane  $z = s_1x + s_2y + t$

$$\tau^3(s_1, s_2, u, v) = s_1u + s_2v. \tag{3.28}$$

**Notation.** Let

$$\dot{I}^1 = E^1 I, \quad \dot{I}^2 = E^2 I, \quad \dot{I}^3 = E^3 I.$$

**Definition 3.6** (*Shearing operators*). The three “shearing operators”

$$S_{s_1, s_2}^1 : \mathbb{I}_{m \times n \times n} \rightarrow \mathbb{I}_{m \times n \times n}, \quad S_{s_1, s_2}^2 : \mathbb{I}_{n \times m \times n} \rightarrow \mathbb{I}_{n \times m \times n}, \quad S_{s_1, s_2}^3 : \mathbb{I}_{n \times n \times m} \rightarrow \mathbb{I}_{n \times n \times m}$$

with  $m = 3n + 1$  are defined by

$$(S_{s_1, s_2}^1 I)(u, v, w) = (T_{-\tau^1(s_1, s_2, v, w)} I(\cdot, v, w))_u, \tag{3.29}$$

$$(S_{s_1, s_2}^2 I)(u, v, w) = (T_{-\tau^2(s_1, s_2, u, w)} I(u, \cdot, w))_v, \tag{3.30}$$

$$(S_{s_1, s_2}^3 I)(u, v, w) = (T_{-\tau^3(s_1, s_2, u, v)} I(u, v, \cdot))_w, \tag{3.31}$$

where  $T_\tau$  is the translation operator given by Eq. (3.1) and  $\tau^1$ ,  $\tau^2$ , and  $\tau^3$  defined in Definition 3.5.

We can use the shearing operator to give an alternative formulation to the 3D Radon transform.

**Lemma 3.4.** For  $z$ -plane whose explicit equation is given by  $z = s_1x + s_2y + t$  we have

$$RI(s_1, s_2, t) = \sum_{u=-n/2}^{n/2-1} \sum_{v=-n/2}^{n/2-1} (S_{s_1, s_2}^3 \dot{I}^3)(u, v, t).$$

**Proof.** By Definition 2.4, for  $z$ -plane, we have

$$RI(s_1, s_2, t) = \sum_{u=-n/2}^{n/2-1} \sum_{v=-n/2}^{n/2-1} \tilde{I}^3(u, v, s_1u + s_2v + t), \tag{3.32}$$

where

$$\tilde{I}^3(u, v, z) = \sum_{w=-n/2}^{n/2-1} I(u, v, w) D_m(z - w), \quad u, v \in \left\{ -\frac{n}{2}, \dots, \frac{n}{2} - 1 \right\}, \quad z \in \mathbb{R}. \tag{3.33}$$

Substituting  $z = s_1u + s_2v + t$  into Eq. (3.33) we get

$$\tilde{I}^3(u, v, s_1u + s_2v + t) = \sum_{w=-n/2}^{n/2-1} I(u, v, w) D_m(s_1u + s_2v + t - w). \quad (3.34)$$

Substituting Eq. (3.34) into Eq. (3.32) we get

$$RI(s_1, s_2, t) = \sum_{u=-n/2}^{n/2-1} \sum_{v=-n/2}^{n/2-1} \sum_{w=-n/2}^{n/2-1} I(u, v, w) D_m(s_1u + s_2v + t - w). \quad (3.35)$$

On the other hand, from Eq. (3.31)

$$\sum_{u=-n/2}^{n/2-1} \sum_{v=-n/2}^{n/2-1} (S_{s_1, s_2}^3 \dot{I}^3)(u, v, t) = \sum_{u=-n/2}^{n/2-1} \sum_{v=-n/2}^{n/2-1} (T_{-\tau^3(s_1, s_2, u, v)} \dot{I}^3(u, v, \cdot))_t. \quad (3.36)$$

From Eq. (3.1) we have

$$T_\tau \dot{I}^3(u, v, \cdot)_t = \sum_{w=-3n/2}^{3n/2} \dot{I}^3(u, v, w) D_m(t - w - \tau), \quad u, v \in \left\{ -\frac{n}{2}, \dots, \frac{n}{2} - 1 \right\}, \quad (3.37)$$

and substituting  $\tau = -\tau^3(s_1, s_2, u, v)$  into Eq. (3.37) we obtain using Eq. (3.28) that

$$\begin{aligned} T_{-\tau^3(s_1, s_2, u, v)} \dot{I}^3(u, v, \cdot)_t &= \sum_{w=-3n/2}^{3n/2} \dot{I}^3(u, v, w) D_m(t - w + s_1u + s_2v) \\ &= \sum_{w=-n/2}^{n/2-1} I(u, v, w) D_m(t - w + s_1u + s_2v). \end{aligned} \quad (3.38)$$

Therefore, substituting Eq. (3.38) into Eq. (3.36) it follows that

$$\begin{aligned} \sum_{u=-n/2}^{n/2-1} \sum_{v=-n/2}^{n/2-1} (S_{s_1, s_2}^3 \dot{I}^3)(u, v, t) &= \sum_{u=-n/2}^{n/2-1} \sum_{v=-n/2}^{n/2-1} (T_{-\tau^3(s_1, s_2, u, v)} \dot{I}^3(u, v, \cdot))_t \\ &= \sum_{u=-n/2}^{n/2-1} \sum_{v=-n/2}^{n/2-1} \sum_{w=-n/2}^{n/2-1} I(u, v, w) D_m(t - w + s_1u + s_2v). \end{aligned}$$

Hence, for  $z$ -plane whose equation is  $z = s_1x + s_2y + t$

$$RI(s_1, s_2, t) = \sum_{u=-n/2}^{n/2-1} \sum_{v=-n/2}^{n/2-1} (S_{s_1, s_2}^3 \dot{I}^3)(u, v, t). \quad \square$$

By repeating the proof for  $x, y$ -planes, we prove the following theorem:

**Theorem 3.5.** *Given a plane  $p$ , one of the following holds:*

(1) If  $C(p)$  is  $x$ -plane given by  $x = s_1y + s_2z + t$  then

$$R_{s_1,s_2}I(t) \triangleq RI(s_1, s_2, t) = \sum_{v=-n/2}^{n/2-1} \sum_{w=-n/2}^{n/2-1} (S_{s_1,s_2}^1 \dot{I}^1)(t, v, w);$$

(2) If  $C(p)$  is  $y$ -plane given by  $y = s_1x + s_2z + t$  then

$$R_{s_1,s_2}I(t) \triangleq RI(s_1, s_2, t) = \sum_{u=-n/2}^{n/2-1} \sum_{w=-n/2}^{n/2-1} (S_{s_1,s_2}^2 \dot{I}^2)(u, t, w);$$

(3) If  $C(p)$  is  $z$ -plane given by  $z = s_1x + s_2y + t$  then

$$R_{s_1,s_2}I(t) \triangleq RI(s_1, s_2, t) = \sum_{u=-n/2}^{n/2-1} \sum_{v=-n/2}^{n/2-1} (S_{s_1,s_2}^3 \dot{I}^3)(u, v, t),$$

where  $C(p)$  is the canonization transform defined in Definition 2.3.

**Definition 3.7** (Backprojection operators). Let  $\psi = (\psi_t : -3n/2 \leq t \leq 3n/2)$  be a vector. The operators  $B_{s_1,s_2}^i$  ( $i = 1, 2, 3$ )

$$B_{s_1,s_2}^1 : \mathbb{C}^m \rightarrow \mathbb{I}_{m \times n \times n}, \quad B_{s_1,s_2}^2 : \mathbb{C}^m \rightarrow \mathbb{I}_{n \times m \times n}, \quad B_{s_1,s_2}^3 : \mathbb{C}^m \rightarrow \mathbb{I}_{n \times n \times m}$$

are defined by

$$(B_{s_1,s_2}^1 \psi)(u, v, w) = (T_{\tau^1(s_1,s_2,v,w)} \psi)(u), \tag{3.39}$$

$$(B_{s_1,s_2}^2 \psi)(u, v, w) = (T_{\tau^2(s_1,s_2,u,w)} \psi)(v), \tag{3.40}$$

$$(B_{s_1,s_2}^3 \psi)(u, v, w) = (T_{\tau^3(s_1,s_2,u,v)} \psi)(w). \tag{3.41}$$

**Lemma 3.6.**

$$\text{adj } B_{s_1,s_2}^1 = \sum_{v,w} S_{s_1,s_2}^1, \quad \text{adj } B_{s_1,s_2}^2 = \sum_{u,w} S_{s_1,s_2}^2, \quad \text{adj } B_{s_1,s_2}^3 = \sum_{u,v} S_{s_1,s_2}^3.$$

The domain and the range of  $\text{adj } B_{s_1,s_2}^i$  is

$$\text{adj } B_{s_1,s_2}^1 : \mathbb{I}_{m \times n \times n} \rightarrow \mathbb{C}^m, \quad \text{adj } B_{s_1,s_2}^2 : \mathbb{I}_{n \times m \times n} \rightarrow \mathbb{C}^m, \quad \text{adj } B_{s_1,s_2}^3 : \mathbb{I}_{n \times n \times m} \rightarrow \mathbb{C}^m.$$

**Proof.** Consider  $B_{s_1,s_2}^3$ . Let  $I^3 \in \mathbb{I}_{n \times n \times m}$  and  $\psi \in \mathbb{C}^m$ . Then,

$$\begin{aligned} \left\langle \sum_{u=-n/2}^{n/2-1} \sum_{v=-n/2}^{n/2-1} (S_{s_1,s_2}^3 I^3)(u, v, \cdot), \psi \right\rangle &= \sum_{u=-n/2}^{n/2-1} \sum_{v=-n/2}^{n/2-1} \langle (S_{s_1,s_2}^3 I^3)(u, v, \cdot), \psi \rangle \\ &= \sum_{u=-n/2}^{n/2-1} \sum_{v=-n/2}^{n/2-1} \langle T_{-\tau^3(s_1,s_2,u,v)} I^3(u, v, \cdot), \psi \rangle \quad (\text{by Eq. (3.31)}) \\ &= \sum_{u=-n/2}^{n/2-1} \sum_{v=-n/2}^{n/2-1} \langle I^3(u, v, \cdot), T_{\tau^3(s_1,s_2,u,v)} \psi \rangle \quad (\text{by Lemma 3.1}) \end{aligned}$$

$$\begin{aligned}
&= \sum_{u=-n/2}^{n/2-1} \sum_{v=-n/2}^{n/2-1} \langle I^3(u, v, \cdot), (B_{s_1, s_2}^3 \psi)(u, v, \cdot) \rangle \quad (\text{by Eq. (3.41)}) \\
&= \sum_{u=-n/2}^{n/2-1} \sum_{v=-n/2}^{n/2-1} \sum_{w=-3n/2}^{3n/2} I^3(u, v, w) (B_{s_1, s_2}^3 \psi(u, v, w))^* = \langle I, B_{s_1, s_2}^3 \psi \rangle.
\end{aligned}$$

Then,

$$\text{adj } B_{s_1, s_2}^3 = \sum_{u, v} S_{s_1, s_2}^3.$$

The proofs for  $B_{s_1, s_2}^1$  and  $B_{s_1, s_2}^2$  are similar.  $\square$

From Theorem 3.5 we have that for an  $x$ -plane

$$R_{s_1, s_2} I = \left( \sum_{v, w} S_{s_1, s_2}^1 E^1 I \right).$$

Hence, we can write the adjoint Radon transform operator as

$$\text{adj } R_{s_1, s_2} = \text{adj } E^1 \circ \text{adj} \left( \sum_{v, w} S_{s_1, s_2}^1 \right).$$

Using Lemmas 3.3 and 3.6 we obtain for  $x$ -plane

$$\text{adj } R_{s_1, s_2} = U^1 \circ B_{s_1, s_2}^1. \quad (3.42)$$

Similarly, we have for the  $y$ -plane

$$\text{adj } R_{s_1, s_2} = U^2 \circ B_{s_1, s_2}^2 \quad (3.43)$$

and for the  $z$ -plane

$$\text{adj } R_{s_1, s_2} = U^3 \circ B_{s_1, s_2}^3. \quad (3.44)$$

Since

$$B_{s_1, s_2}^1 : \mathbb{C}^m \rightarrow \mathbb{I}_{m \times n \times n} \quad (m = 3n + 1)$$

and

$$U^1 : \mathbb{I}_{m \times n \times n} \rightarrow \mathbb{I}_{n \times n \times n}$$

it follows that

$$\text{adj } R_{s_1, s_2} : \mathbb{C}^m \rightarrow \mathbb{I}_{n \times n \times n}.$$

We will use the adjoint Radon transform to analyze the projections of the Radon transform on the exponentials  $\varphi^{(k)}(t) = e^{2\pi i kt/m}$ , where  $k \in \mathbb{Z}$ ,  $-3n/2 \leq k \leq 3n/2$ . Define a vector of samples from  $\varphi^{(k)}(t)$  by

$$\phi^{(k)} = \left( \varphi^{(k)} \left( -\frac{3n}{2} \right), \dots, \varphi^{(k)} \left( \frac{3n}{2} \right) \right).$$

Since  $\phi^{(k)}$  is a vector of exponentials, by Lemma 3.2 it follows that

$$(T_\tau \phi^{(k)})_t = \varphi^{(k)}(t - \tau) \tag{3.45}$$

and by substituting  $\tau^1$ ,  $\tau^2$ , and  $\tau^3$  from Definition 3.5 into Eq. (3.45) we obtain

$$(T_{\tau^1(s_1, s_2, v, w)} \phi^{(k)})(u) = \varphi^{(k)}(u - \tau^1(s_1, s_2, v, w)) = e^{(2\pi i k/m)(u - \tau^1(s_1, s_2, v, w))}, \tag{3.46}$$

$$(T_{\tau^2(s_1, s_2, u, w)} \phi^{(k)})(v) = \varphi^{(k)}(v - \tau^2(s_1, s_2, u, w)) = e^{(2\pi i k/m)(v - \tau^2(s_1, s_2, u, w))}, \tag{3.47}$$

$$(T_{\tau^3(s_1, s_2, u, v)} \phi^{(k)})(w) = \varphi^{(k)}(w - \tau^3(s_1, s_2, u, v)) = e^{(2\pi i k/m)(w - \tau^3(s_1, s_2, u, v))}. \tag{3.48}$$

For  $(s_1, s_2)$  slopes of an  $x$ -plane we have

$$\begin{aligned} \widehat{RI}(s_1, s_2, k) &= \sum_{t=-3n/2}^{3n/2} RI(s_1, s_2, t) e^{-2\pi i k t/m} = \langle RI(s_1, s_2, \cdot), \phi^{(k)} \rangle = \langle I, (\text{adj } R_{s_1, s_2}) \phi^{(k)} \rangle \\ &= \langle I, U^1 B_{s_1, s_2}^1 \phi^{(k)} \rangle \quad (\text{by Eq. (3.42)}) \\ &= \sum_{v, w=-n/2}^{n/2-1} \sum_{u=-n/2}^{n/2-1} I(u, v, w) (T_{\tau^1(s_1, s_2, v, w)} \phi^{(k)})^*(u) \quad (\text{by Eq. (3.39)}) \\ &= \sum_{v, w=-n/2}^{n/2-1} \sum_{u=-n/2}^{n/2-1} I(u, v, w) e^{(-2\pi i k/m)(u - \tau^1(s_1, s_2, v, w))} \quad (\text{by Eq. (3.46)}) \\ &= \sum_{v, w=-n/2}^{n/2-1} \sum_{u=-n/2}^{n/2-1} I(u, v, w) e^{(-2\pi i k/m)(u - s_1 v - s_2 w)} \quad (\text{by Eq. (3.26)}) \\ &= \hat{I}(k, -s_1 k, -s_2 k), \end{aligned}$$

where  $k \in \{-3n/2, \dots, 3n/2\}$  and  $\hat{I}$  is the trigonometric polynomial

$$\hat{I}(\xi_1, \xi_2, \xi_3) = \sum_{u=-n/2}^{n/2-1} \sum_{v=-n/2}^{n/2-1} \sum_{w=-n/2}^{n/2-1} I(u, v, w) e^{(-2\pi i/m)(\xi_1 u + \xi_2 v + \xi_3 w)}. \tag{3.49}$$

We established the 3D Fourier slice theorem for  $x$ -planes

$$\widehat{RI}(s_1, s_2, k) = \hat{I}(k, -s_1 k, -s_2 k) \tag{3.50}$$

that says that the 1D Fourier transform of our Radon transform for fixed direction  $(s_1, s_2)$  equals to the samples of  $\hat{I}$  along the line whose direction vector is  $(1, -s_1, -s_2)$  at  $(k, -s_1 k, -s_2 k)$ ,  $k = -3n/2, \dots, 3n/2$ .

For slopes  $(s_1, s_2)$  of a  $y$ -plane we have

$$\begin{aligned} \widehat{RI}(s_1, s_2, k) &= \sum_{t=-3n/2}^{3n/2} RI(s_1, s_2, t) e^{-2\pi i k t/m} = \langle RI(s_1, s_2, \cdot), \phi^{(k)} \rangle = \langle I, (\text{adj } R_{s_1, s_2}) \phi^{(k)} \rangle \\ &= \langle I, U^2 B_{s_1, s_2}^2 \phi^{(k)} \rangle \quad (\text{by Eq. (3.43)}) \end{aligned}$$

$$\begin{aligned}
&= \sum_{u,w=-n/2}^{n/2-1} \sum_{v=-n/2}^{n/2-1} I(u, v, w) (T_{\tau^2(s_1, s_2, u, w)} \phi^{(k)})^*(v) \quad (\text{by Eq. (3.40)}) \\
&= \sum_{u,w=-n/2}^{n/2-1} \sum_{v=-n/2}^{n/2-1} I(u, v, w) e^{(-2\pi i k/m)(v-\tau^2(s_1, s_2, u, w))} \quad (\text{by Eq. (3.47)}) \\
&= \sum_{u,w=-n/2}^{n/2-1} \sum_{v=-n/2}^{n/2-1} I(u, v, w) e^{(-2\pi i k/m)(v-s_1 u-s_2 w)} \quad (\text{by Eq. (3.27)}) \\
&= \hat{I}(-s_1 k, k, -s_2 k),
\end{aligned}$$

where  $k \in \{-3n/2, \dots, 3n/2\}$  and  $\hat{I}$  is the trigonometric polynomial given in Eq. (3.49).

Thus, for a  $y$ -plane with slopes  $(s_1, s_2)$  we have

$$\widehat{RI}(s_1, s_2, k) = \hat{I}(-s_1 k, k, -s_2 k). \quad (3.51)$$

Finally, for slopes  $(s_1, s_2)$  of  $z$ -plane we have

$$\begin{aligned}
\widehat{RI}(s_1, s_2, k) &= \sum_{t=-3n/2}^{3n/2} RI(s_1, s_2, t) e^{-2\pi i k t/m} = \langle RI(s_1, s_2, \cdot), \phi^{(k)} \rangle = \langle I, (\text{adj } R_{s_1, s_2}) \phi^{(k)} \rangle \\
&= \langle I, U^3 B_{s_1, s_2}^3 \phi^{(k)} \rangle \quad (\text{by Eq. (3.44)}) \\
&= \sum_{u,v=-n/2}^{n/2-1} \sum_{w=-n/2}^{n/2-1} I(u, v, w) (T_{\tau^3(s_1, s_2, u, v)} \phi^{(k)})^*(w) \quad (\text{by Eq. (3.41)}) \\
&= \sum_{u,v=-n/2}^{n/2-1} \sum_{w=-n/2}^{n/2-1} I(u, v, w) e^{(-2\pi i k/m)(w-\tau^3(s_1, s_2, u, v))} \quad (\text{by Eq. (3.48)}) \\
&= \sum_{u,v=-n/2}^{n/2-1} \sum_{w=-n/2}^{n/2-1} I(u, v, w) e^{(-2\pi i k/m)(w-s_1 u-s_2 v)} \quad (\text{by Eq. (3.28)}) \\
&= \hat{I}(-s_1 k, -s_2 k, k),
\end{aligned}$$

where  $k \in \{-3n/2, \dots, 3n/2\}$  and  $\hat{I}$  is the trigonometric polynomial given by Eq. (3.49).

For a  $z$ -plane with slopes  $(s_1, s_2)$  we have

$$\widehat{RI}(s_1, s_2, k) = \hat{I}(-s_1 k, -s_2 k, k). \quad (3.52)$$

We proved the following theorem:

**Theorem 3.7** (3D Fourier slice theorem). *Given a 3D image  $I \in \mathbb{I}_{n \times n \times n}$  and a plane  $p$  with  $C(p) = (q, s_1, s_2, t)$ ,  $|s_1| \leq 1$ ,  $|s_2| \leq 1$ ,  $t \in \{-3n/2, \dots, 3n/2\}$  (defined in Definition 2.3), then*

$$\widehat{RI}(s_1, s_2, k) = \begin{cases} \hat{I}(k, -s_1 k, -s_2 k), & q = 1, \\ \hat{I}(-s_1 k, k, -s_2 k), & q = 2, \\ \hat{I}(-s_1 k, -s_2 k, k), & q = 3, \end{cases} \quad (3.53)$$

where  $\widehat{RI}$  is the 1D Fourier of  $RI$  along the parameter  $t$

$$\widehat{RI}(s_1, s_2, k) = \sum_{t=-3n/2}^{3n/2} RI(s_1, s_2, t)e^{-2\pi i kt/m}, \quad k \in \mathbb{Z}, \quad -3n/2 \leq k \leq 3n/2$$

and

$$\hat{I}(\xi_1, \xi_2, \xi_3) = \sum_{u=-n/2}^{n/2-1} \sum_{v=-n/2}^{n/2-1} \sum_{w=-n/2}^{n/2-1} I(u, v, w)e^{(-2\pi i/m)(\xi_1 u + \xi_2 v + \xi_3 w)}.$$

#### 4. 3D pseudo-polar grid

The Fourier slice Theorem 3.7 establishes the relation between the 1D DFT of the Radon transform  $RI$  given by Eq. (2.15) and the trigonometric polynomial

$$\hat{I}(\xi_1, \xi_2, \xi_3) = \sum_{u=-n/2}^{n/2-1} \sum_{v=-n/2}^{n/2-1} \sum_{w=-n/2}^{n/2-1} I(u, v, w)e^{(-2\pi i/m)(\xi_1 u + \xi_2 v + \xi_3 w)}, \quad m = 3n + 1. \quad (4.1)$$

$RI$  is defined for continuous slopes  $(s_1, s_2)$  in  $[-1, 1] \times [-1, 1]$  while  $I$  is discrete. We would like to discretize  $s_1$  and  $s_2$  while satisfying properties (P1)–(P5) (Section 1.2).

We define three sets

$$S_1 \triangleq \left\{ \frac{l}{n/2} \mid l = -\frac{n}{2}, \dots, \frac{n}{2} \right\}, \quad S_2 \triangleq \left\{ \frac{j}{n/2} \mid j = -\frac{n}{2}, \dots, \frac{n}{2} \right\},$$

$$T \triangleq \left\{ t \in \mathbb{Z} \mid -\frac{3n}{2} \leq t \leq \frac{3n}{2} \right\}.$$

The 3D discrete Radon transform will be defined as the restriction of  $RI$  (Definition 2.4) to the set of slopes  $(s_1, s_2) \in S_1 \times S_2$  with  $t \in T$ .

By restricting  $s_1$  and  $s_2$  we defined a discrete set of planes over which we sum (interpolated) samples of  $I$ . More specifically, in our definition of the 3D Radon transform as summation over planes of the interpolated values of the image  $I$ , we sum over the following planes:

- All  $x$ -planes  $x = s_1 y + s_2 z + t$ , where  $(s_1, s_2) \in S_1 \times S_2, t \in T$ ;
- All  $y$ -planes  $y = s_1 x + s_2 z + t$ , where  $(s_1, s_2) \in S_1 \times S_2, t \in T$ ;
- All  $z$ -planes  $z = s_1 x + s_2 y + t$ , where  $(s_1, s_2) \in S_1 \times S_2, t \in T$ .

The slopes in each direction in the described planes are equally spaced.

**Definition 4.1** (3D discrete Radon transform). Given a plane  $p$  whose canonized form is  $C(p) = (q, s_1, s_2, t)$  with slopes  $(s_1, s_2) \in S_1 \times S_2, t \in T$ , then

$$RI(s_1, s_2, t) \triangleq \begin{cases} R_1 I(s_1, s_2, t), & q = 1, \\ R_2 I(s_1, s_2, t), & q = 2, \\ R_3 I(s_1, s_2, t), & q = 3, \end{cases} \quad (4.2)$$

where  $R_1 I, R_2 I$ , and  $R_3 I$  are defined in Definition 2.4.

$RI$  is not defined for every plane  $p$ , but only for planes  $p$  such that for  $C(p) = (q, s_1, s_2, t)$  it holds that  $(s_1, s_2) \in S_1 \times S_2$  and  $t \in T$ . The difference between Definitions 2.4 and 4.1 is in the discrete set of slopes  $S_1 \times S_2$ . It replaces the continuous set of slopes  $[-1, 1] \times [-1, 1]$ . Definition 4.1 describes a transform that takes an image  $I$  of size  $n^3$  into an array of size  $3 \times (3n + 1) \times (n + 1)^2$ .

The Fourier slice Theorem 3.7 holds also for the discrete set of slopes  $S_1 \times S_2$  for each of the plane types:

- For an  $x$ -plane

$$\widehat{RI}\left(\frac{2l}{n}, \frac{2j}{n}, k\right) = \hat{I}\left(k, -\frac{2l}{n}k, -\frac{2j}{n}k\right), \quad l, j \in \left\{-\frac{n}{2}, \dots, \frac{n}{2}\right\}, \quad k \in \left\{-\frac{3n}{2}, \dots, \frac{3n}{2}\right\}. \quad (4.3)$$

- For a  $y$ -plane

$$\widehat{RI}\left(\frac{2l}{n}, \frac{2j}{n}, k\right) = \hat{I}\left(-\frac{2l}{n}k, k, -\frac{2j}{n}k\right), \quad l, j \in \left\{-\frac{n}{2}, \dots, \frac{n}{2}\right\}, \quad k \in \left\{-\frac{3n}{2}, \dots, \frac{3n}{2}\right\}. \quad (4.4)$$

- For a  $z$ -plane

$$\widehat{RI}\left(\frac{2l}{n}, \frac{2j}{n}, k\right) = \hat{I}\left(-\frac{2l}{n}k, -\frac{2j}{n}k, k\right), \quad l, j \in \left\{-\frac{n}{2}, \dots, \frac{n}{2}\right\}, \quad k \in \left\{-\frac{3n}{2}, \dots, \frac{3n}{2}\right\}, \quad (4.5)$$

where  $\hat{I}$  is the trigonometric polynomial given by Eq. (4.1).

Next we will describe how the samples of  $\hat{I}$  in Eqs. (4.3)–(4.5) are scattered in the space  $\mathbb{R}^3$ . In order to obtain  $\widehat{RI}$  over all  $x$ -planes, by Eq. (4.3) we sample  $\hat{I}$  at

$$P_1 \triangleq \left\{ \left( k, -\frac{2l}{n}k, -\frac{2j}{n}k \right) \mid l, j \in \left\{-\frac{n}{2}, \dots, \frac{n}{2}\right\}, \quad k \in \left\{-\frac{3n}{2}, \dots, \frac{3n}{2}\right\} \right\}.$$

Similarly, to obtain  $\widehat{RI}$  over all  $y$ -planes, by Eq. (4.4) we sample  $\hat{I}$  at

$$P_2 \triangleq \left\{ \left( -\frac{2l}{n}k, k, -\frac{2j}{n}k \right) \mid l, j \in \left\{-\frac{n}{2}, \dots, \frac{n}{2}\right\}, \quad k \in \left\{-\frac{3n}{2}, \dots, \frac{3n}{2}\right\} \right\}$$

and finally, to obtain  $\widehat{RI}$  over all  $z$ -planes, by Eq. (4.5) we sample  $\hat{I}$  at

$$P_3 \triangleq \left\{ \left( -\frac{2l}{n}k, -\frac{2j}{n}k, k \right) \mid l, j \in \left\{-\frac{n}{2}, \dots, \frac{n}{2}\right\}, \quad k \in \left\{-\frac{3n}{2}, \dots, \frac{3n}{2}\right\} \right\}.$$

The set

$$P \triangleq P_1 \cup P_2 \cup P_3$$

is called the *pseudo-polar grid*. See Figs. 7–10 for illustrations of the sets  $P_1$ ,  $P_2$ ,  $P_3$ , and  $P$ .

The pseudo-polar Fourier transform is defined by sampling the trigonometric polynomial  $\hat{I}$  on the pseudo-polar grid  $P$ .

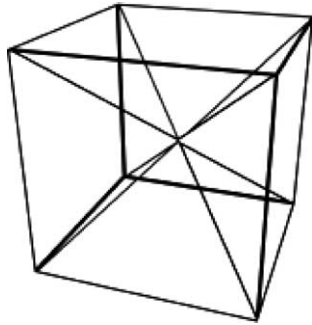


Fig. 7. Illustration of the 3D pseudo-polar grid.

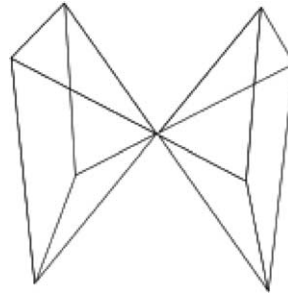


Fig. 8. The sector  $P_1$ .

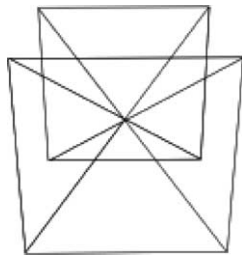


Fig. 9. The sector  $P_2$ .

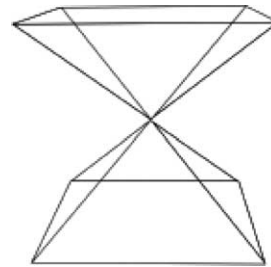


Fig. 10. The sector  $P_3$ .

**Definition 4.2** (*Pseudo-polar Fourier transform*). The pseudo-polar Fourier transform  $PP_i$  ( $i = 1, 2, 3$ ) is a linear transformation from 3D images  $I \in \mathbb{I}_{n \times n \times n}$  defined by

$$\begin{aligned}
 PP_1 I(k, l, j) &= \hat{I}\left(k, -\frac{2l}{n}k, -\frac{2j}{n}k\right), & PP_2 I(k, l, j) &= \hat{I}\left(-\frac{2l}{n}k, k, -\frac{2j}{n}k\right), \\
 PP_3 I(k, l, j) &= \hat{I}\left(-\frac{2l}{n}k, -\frac{2j}{n}k, k\right),
 \end{aligned}
 \tag{4.6}$$

where

$$l, j \in \left\{-\frac{n}{2}, \dots, \frac{n}{2}\right\}, \quad k \in \left\{-\frac{3n}{2}, \dots, \frac{3n}{2}\right\}, \quad m = 3n + 1$$

and

$$\hat{I}(\xi_1, \xi_2, \xi_3) = \sum_{u=-n/2}^{n/2-1} \sum_{v=-n/2}^{n/2-1} \sum_{w=-n/2}^{n/2-1} I(u, v, w) e^{(-2\pi i/m)(\xi_1 u + \xi_2 v + \xi_3 w)}.$$

Using the pseudo-polar Fourier transform we can express  $RI$  as

$$R_i I = F^{-1} \circ PP_i I \quad (i = 1, 2, 3),
 \tag{4.7}$$

where  $F^{-1}$  is the inverse Fourier transform.

We can regard  $s_1$  and  $s_2$  as “pseudo-angles” and  $k$  as a “pseudo-radius”. This corresponds to the  $(r, \phi, \theta)$  representation of the polar grid.

## 5. Rapid computation of the 3D discrete Radon transform

We will show that the 3D discrete Radon transform can be computed by an  $O(n^3 \log n)$  algorithm.

Let  $F^{-1}$  be the 1D inverse Fourier transform. From Eq. (4.7)

$$R_i I = F^{-1} \circ P P_i I \quad (i = 1, 2, 3), \quad (5.1)$$

we see that it is being called  $(n + 1)^2$  times for each  $P P_i I$ . Each vector in  $P P_i I$  corresponds to fixed slopes  $l, j$ . Hence, all applications of  $F^{-1}$  take  $O(n^3 \log n)$  operations. Remains to show that the 3D pseudo-polar Fourier transform  $P P_i I$  ( $i = 1, 2, 3$ ) can be computed in  $O(n^3 \log n)$  operations as the standard 3D FFT.

From Definition 4.2 it follows that for a given image  $I \in \mathbb{I}_{n \times n \times n}$ , the pseudo-polar Fourier transform of  $I$  is defined by

$$P P I(s, k, l, j) = \begin{cases} \hat{I}(k, -\frac{2l}{n}k, -\frac{2j}{n}k) & (s = 1) \\ \hat{I}(-\frac{2l}{n}k, k, -\frac{2j}{n}k) & (s = 2) \\ \hat{I}(-\frac{2l}{n}k, -\frac{2j}{n}k, k) & (s = 3) \end{cases} = \begin{cases} P P_1 I(k, l, j), \\ P P_2 I(k, l, j), \\ P P_3 I(k, l, j), \end{cases} \quad (5.2)$$

where

$$l, j \in \left\{ -\frac{n}{2}, \dots, \frac{n}{2} \right\}, \quad k \in \left\{ -\frac{3n}{2}, \dots, \frac{3n}{2} \right\}, \quad m = 3n + 1$$

and

$$\hat{I}(\xi_1, \xi_2, \xi_3) = \sum_{u=-n/2}^{n/2-1} \sum_{v=-n/2}^{n/2-1} \sum_{w=-n/2}^{n/2-1} I(u, v, w) e^{(-2\pi i/m)(\xi_1 u + \xi_2 v + \xi_3 w)}.$$

We will show that for a given image  $I$ , we can rapidly resample  $\hat{I}$  on the pseudo-polar grid points. The operator behind this resampling process is the *fractional Fourier transform*.

**Definition 5.1** (*Fractional Fourier transform*). Given a vector  $X$ ,  $X = (X(j), -n/2 \leq j \leq n/2)$ , and an arbitrary  $\alpha \in \mathbb{R}$ , the fractional Fourier transform is defined as

$$(F_{n+1}^\alpha X)(\omega) = \sum_{u=-n/2}^{n/2} X(u) e^{-2\pi i \alpha \omega u / (n+1)}, \quad \omega \in \mathbb{Z}, \quad -n/2 \leq \omega \leq n/2. \quad (5.3)$$

An important property of the fractional Fourier transform defined in Definition 5.1 is that for a given vector  $\{X(j)\}$  of  $n + 1$  numbers, the sequence  $(F_{n+1}^\alpha X)(\omega)$  can be computed using  $O(n \log n)$  operations for any  $\alpha \in \mathbb{R}$  (see [7]).

The main idea behind the algorithm for the computation of the 3D pseudo-polar Fourier transform is to use the samples of the equally spaced 3D DFT (which can be computed in  $O(n^3 \log n)$ ), and resample them rapidly on the pseudo-polar grid points, using the fractional Fourier transform.

We first give the pseudo-code for the algorithm that computes  $PPI$ , then a proof of its correctness will be given, and finally, the time complexity of the algorithm will be analyzed.

Throughout this section we will use the following notation:

**Notation 1.**  $F_n^{-1}$ . 1D inverse DFT.

$F_m^\alpha$ . Fractional Fourier transform with factor  $\alpha$ . The operator accepts a sequence of length  $n$ , pads it symmetrically to length  $m = 3n + 1$ , applies to it the fractional Fourier transform with factor  $\alpha$ , and returns the  $n + 1$  central elements.

$F_3$ . 3D DFT.

$G_{k,n}$ . Consecutive application of  $F_n^{-1}$  followed by  $F_m^{2k/n}$ :

$$G_{k,n} \triangleq F_m^{2k/n} \circ F_n^{-1}.$$

### 5.1. Algorithm description for the rapid computation of the 3D pseudo-polar Fourier transform (pseudo-code)

**Input:** Image  $I$  of size  $n \times n \times n$ .

**Output:** Three arrays,  $\text{Res}_1$ ,  $\text{Res}_2$ , and  $\text{Res}_3$ , of size  $m \times (n + 1) \times (n + 1)$ .

**Working arrays:** Six auxiliary arrays  $T_1, T_2, T_3, T'_1, T'_2, T'_3$ :

- $T_1$  is of size  $m \times n \times (n + 1)$ ;
- $T_2$  is of size  $(n + 1) \times m \times n$ ;
- $T_3$  is of size  $n \times (n + 1) \times m$ ;
- $T'_1, T'_2, T'_3$  are of size  $m \times (n + 1) \times (n + 1)$ .

**Process:**  $\text{Res}_1$  **computation:**

(1)  $\hat{I}_d \leftarrow F_3(E^1 I)$ . 3D DFT of  $I$  padded to length  $m$  in the  $x$ -direction where  $E^1$  was defined in Definition 3.3.

(2) For each  $k$  and  $l$

$$U = \hat{I}_d(k, l, \cdot)$$

and compute

$$T_1(k, l, \cdot) = G_{k,n} U.$$

(3) For each  $k$  and  $j$

$$V = T_1(k, \cdot, j)$$

and compute

$$T'_1(k, \cdot, j) = G_{k,n} V.$$

(4) For each  $k, l, j$

$$\text{Res}_1(k, l, j) = T'_1(k, -l, -j).$$

The following steps resemble the steps (1)–(4) above while  $\text{Res}_2$  and  $\text{Res}_3$  are used instead of  $\text{Res}_1$ .

**Res<sub>2</sub> computation:**

(5)  $\hat{I}_d \leftarrow F_3(E^2 I)$ . 3D DFT of  $I$  padded to length  $m$  in the  $y$ -direction where  $E^2$  was defined in Definition 3.3.

(6) For each  $k$  and  $l$

$$U = \hat{I}_d(\cdot, k, j)$$

and compute

$$T_2(\cdot, k, j) = G_{k,n} U.$$

(7) For each  $k$  and  $j$

$$V = T_2(l, k, \cdot)$$

and compute

$$T'_2(k, l, \cdot) = G_{k,n} V.$$

(8) For each  $k, l, j$

$$\text{Res}_2(k, l, j) = T'_2(k, -l, -j).$$

**Res<sub>3</sub> computation:**

(9)  $\hat{I}_d \leftarrow F_3(E^3 I)$ . 3D DFT of  $I$  padded to length  $m$  in the  $z$ -direction where  $E^3$  was defined in Definition 3.3.

(10) For each  $k$  and  $l$

$$U = \hat{I}_d(l, \cdot, k)$$

and compute

$$T_3(l, \cdot, k) = G_{k,n} U.$$

(11) For each  $k$  and  $j$

$$V = T_3(\cdot, j, k)$$

and compute

$$T'_3(k, \cdot, j) = G_{k,n} V.$$

(12) For each  $k, l, j$

$$\text{Res}_3(k, l, j) = T'_3(k, -l, -j).$$

**5.2. Algorithm 5.1 correctness**

To illustrate the flow of the algorithm we show its operations on Res<sub>3</sub>.

- (1) Both ends of the  $z$ -direction of the image  $I$  are zero padded. The 3D DFT of the padded image is computed. The results are placed in  $\hat{I}_d$ . See Figs. 11(a) and 11(b).
- (2) Take each vector from  $\hat{I}_d$ , which corresponds to fixed  $x$  and  $z$ . Apply on it the 1D inverse DFT and resample it using 1D fractional Fourier transform where  $\alpha = 2z/n$ . The result 3D array is denoted by  $T_3$ . See Fig. 11(c).

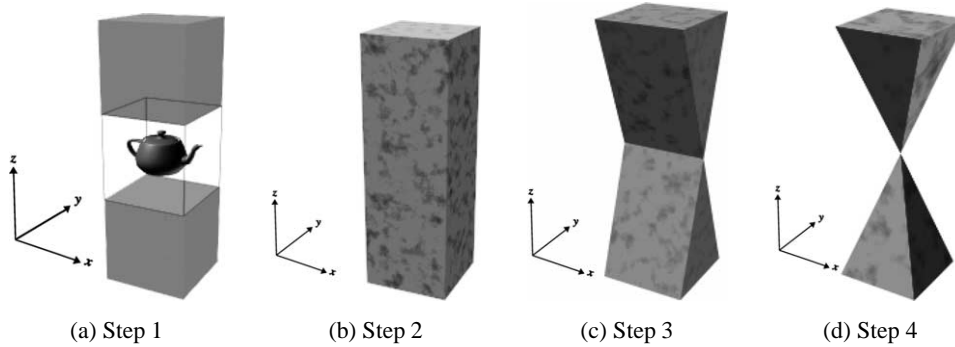


Fig. 11. Illustrating the computation of Res<sub>3</sub>.

- (3) Take each vector from  $T_3$ , which corresponds to fixed  $y$  and  $z$ . Apply on it 1D inverse DFT and resample it using 1D fractional Fourier transform where  $\alpha = 2z/n$ . The result array is  $T'_3$ . See Fig. 11(d).
- (4) Flip  $T'_3$  along the  $y$ - and  $z$ -axis.

The indices in Res<sub>1</sub>, Res<sub>2</sub>, and Res<sub>3</sub> have the following meaning:

- Res<sub>1</sub>( $k, l, j$ )  $k$  pseudo-radius (unit steps in  $x$ -direction),  
 $l$  pseudo-angle in  $y$ -direction,  
 $j$  pseudo-angle in  $z$ -direction;
- Res<sub>2</sub>( $k, l, j$ )  $k$  pseudo-radius (unit steps in  $y$ -direction),  
 $l$  pseudo-angle in  $x$ -direction,  
 $j$  pseudo-angle in  $z$ -direction;
- Res<sub>3</sub>( $k, l, j$ )  $k$  pseudo-radius (unit steps in  $z$ -direction),  
 $l$  pseudo-angle in  $x$ -direction,  
 $j$  pseudo-angle in  $y$ -direction.

**Theorem 5.1** (Algorithm correctness).

- Res<sub>1</sub>( $k, l, j$ ) =  $PPI(1, k, l, j)$ ;
- Res<sub>2</sub>( $k, l, j$ ) =  $PPI(2, k, l, j)$ ;
- Res<sub>3</sub>( $k, l, j$ ) =  $PPI(3, k, l, j)$ .

We will prove the correctness of the algorithm only for Res<sub>1</sub> (steps (1)–(4) of Algorithm 5.1). The proofs for Res<sub>2</sub> and Res<sub>3</sub> are the same.

**Proof.** After step (1) of Algorithm 5.1 we have

$$\hat{I}_d(\xi_1, \xi_2, \xi_3) = \sum_{u=-n/2}^{n/2-1} \sum_{v=-n/2}^{n/2-1} \sum_{w=-n/2}^{n/2-1} I(u, v, w) e^{-2\pi i \xi_1 u/m} e^{-2\pi i \xi_2 v/n} e^{-2\pi i \xi_3 w/n} \tag{5.4}$$

where

$$-\frac{3n}{2} \leq \xi_1 \leq \frac{3n}{2}, \quad -\frac{n}{2} \leq \xi_2, \xi_3 < \frac{n}{2}.$$

We next calculate the entry  $T_1(k, l, j)$ . According to step (2) of Algorithm 5.1, we take a vector  $U$  from  $\hat{I}_d$ , which corresponds to  $\xi_1 = k$ ,  $\xi_2 = l$ , and a variable  $\xi_3$

$$U = \hat{I}_d(k, l, \cdot) \quad (5.5)$$

and apply  $G_{k,n}$  to Eq. (5.5)

$$T_1(k, l, \cdot) = G_{k,n}U = F_m^{2k/n}(F_n^{-1}(U)).$$

By expanding  $U$  using Eq. (5.4) we get

$$\begin{aligned} U(j) = \hat{I}_d(k, l, j) &= \sum_{u=-n/2}^{n/2-1} \sum_{v=-n/2}^{n/2-1} \sum_{w=-n/2}^{n/2-1} I(u, v, w) e^{-2\pi i k u/m} e^{-2\pi i l v/n} e^{-2\pi i j w/n} \\ &= \sum_{w=-n/2}^{n/2-1} \left( \sum_{u=-n/2}^{n/2-1} \sum_{v=-n/2}^{n/2-1} I(u, v, w) e^{-2\pi i k u/m} e^{-2\pi i l v/n} \right) e^{-2\pi i j w/n} \\ &= \sum_{w=-n/2}^{n/2-1} c_{k,l}(w) e^{-2\pi i j w/n}, \end{aligned} \quad (5.6)$$

where

$$c_{k,l}(w) = \sum_{u=-n/2}^{n/2-1} \sum_{v=-n/2}^{n/2-1} I(u, v, w) e^{-2\pi i k u/m} e^{-2\pi i l v/n}. \quad (5.7)$$

As we can see from Eq. (5.6), the vector  $U$  is the DFT of the vector  $\{c_{k,l}(w)\}$ , and therefore

$$F_n^{-1}(U) = \{c_{k,l}(w)\}. \quad (5.8)$$

We next compute the fractional Fourier transform of  $F_n^{-1}(U)$ , i.e., the fractional Fourier transform of the vector  $\{c_{k,l}(w)\}$  with  $\alpha = 2k/n$ . From Eq. (5.8)

$$(F_m^{2k/n}(F_n^{-1}(U)))_j = (F_m^{2k/n}(\{c_{k,l}(w)\}))_j \quad (5.9)$$

$$= \sum_{w=-n/2}^{n/2-1} c_{k,l}(w) e^{-2\pi i (2k/n) j w/m} \quad (5.10)$$

$$= \sum_{w=-n/2}^{n/2-1} \sum_{u=-n/2}^{n/2-1} \sum_{v=-n/2}^{n/2-1} I(u, v, w) e^{-2\pi i k u/m} e^{-2\pi i l v/n} e^{-2\pi i (2k/n) j w/m}, \quad (5.11)$$

where Eq. (5.9) follows from Eq. (5.8), and Eq. (5.11) follows from Eq. (5.7). Thus we have

$$(F_m^{2k/n}(F_n^{-1}U))_j = \sum_{w=-n/2}^{n/2-1} \sum_{u=-n/2}^{n/2-1} \sum_{v=-n/2}^{n/2-1} I(u, v, w) e^{-2\pi i k u/m} e^{-2\pi i l v/n} e^{-2\pi i (2k/n) j w/m}. \quad (5.12)$$

Hence, after step (2) of Algorithm 5.1 we have from Eq. (5.12)

$$\begin{aligned}
 T_1(k, l, j) &= (G_{k,n}U)_j = \left(F_m^{2k/n}(F_n^{-1}(U))\right)_j \\
 &= \sum_{u=-n/2}^{n/2-1} \sum_{v=-n/2}^{n/2-1} \sum_{w=-n/2}^{n/2-1} I(u, v, w)e^{-2\pi iku/m}e^{-2\pi ilv/n}e^{-2\pi i(2k/n)jw/m} \\
 &= \hat{I}\left(k, \frac{lm}{n}, \frac{2jk}{n}\right). \tag{5.13}
 \end{aligned}$$

In order not to confuse with the following references to  $k, l, j$ , we rewrite Eq. (5.13) as

$$T_1(\xi_1, \xi_2, \xi_3) = \hat{I}\left(\xi_1, \frac{\xi_2 n}{m}, \frac{2\xi_1 \xi_3}{n}\right).$$

According to step (3) of Algorithm 5.1, we take a vector  $V$  from  $T_1$ , which corresponds to fixed  $\xi_1 = k$ ,  $\xi_3 = j$ , and a variable  $\xi_2$

$$V = T_1(k, \cdot, j). \tag{5.14}$$

By applying  $G_{k,n}$  to Eq. (5.14) we get

$$T_1'(k, \cdot, j) = G_{k,n}V = F_m^{2k/n}(F_n^{-1}(V)). \tag{5.15}$$

Again, we will first compute  $F_n^{-1}(V)$  and then the  $l$ th element of the vector  $T_1'(k, \cdot, j)$ , i.e., the entry  $T_1'(k, l, j)$ . Using Eq. (5.13)

$$\begin{aligned}
 V(l) = T_1(k, l, j) &= \sum_{u=-n/2}^{n/2-1} \sum_{v=-n/2}^{n/2-1} \sum_{w=-n/2}^{n/2-1} I(u, v, w)e^{-2\pi iku/m}e^{-2\pi ilv/n}e^{-2\pi i(2k/n)jw/m} \\
 &= \sum_{v=-n/2}^{n/2-1} \left( \sum_{u=-n/2}^{n/2-1} \sum_{w=-n/2}^{n/2-1} I(u, v, w)e^{-2\pi iku/m}e^{-2\pi i(2k/n)jw/m} \right) e^{-2\pi ilv/n} \\
 &= \sum_{v=-n/2}^{n/2-1} c_{k,j}(v)e^{-2\pi ilv/n}, \tag{5.16}
 \end{aligned}$$

where

$$c_{k,j}(v) = \sum_{u=-n/2}^{n/2-1} \sum_{w=-n/2}^{n/2-1} I(u, v, w)e^{-2\pi iku/m}e^{-2\pi i(2k/n)jw/m}. \tag{5.17}$$

Equation (5.16) implies that the vector  $V$  is the DFT of the vector  $\{c_{k,j}(v)\}$ , and therefore

$$F_n^{-1}(V) = \{c_{k,j}(v)\}. \tag{5.18}$$

Applying  $F_m^{2k/n}$  to  $F_n^{-1}(V)$  (i.e., to the sequence  $\{c_{k,j}(v)\}$ ) we obtain

$$\begin{aligned}
 \left(F_m^{2k/n}(F_n^{-1}(V))\right)_l &= \left(F_m^{2k/n}(\{c_{k,j}(v)\})\right)_l \\
 &= \sum_{v=-n/2}^{n/2-1} c_{k,j}(v)e^{-2\pi i(2k/n)lv/m} \tag{5.19}
 \end{aligned}$$

$$\begin{aligned}
&= \sum_{u=-n/2}^{n/2-1} \sum_{v=-n/2}^{n/2-1} \sum_{w=-n/2}^{n/2-1} I(u, v, w) e^{-2\pi i k u/m} e^{-2\pi i (2k/n) l v/m} e^{-2\pi i (2k/n) j w/m} \quad (5.20) \\
&= \hat{I}\left(k, \frac{2lk}{n}, \frac{2jk}{n}\right)
\end{aligned}$$

where Eq. (5.19) follows by using Eq. (5.18), and Eq. (5.20) follows by using Eq. (5.17). Hence we have

$$T'_1(k, l, j) = (F_m^{2k/n}(F_n^{-1}(V)))_l = \hat{I}\left(k, \frac{2lk}{n}, \frac{2jk}{n}\right). \quad (5.21)$$

Using Eq. (5.21) we have after step (4) of Algorithm 5.1 (end of computation of  $\text{Res}_1$ ) that

$$\text{Res}_1(k, l, j) = T'_1(k, -l, -j) = \hat{I}\left(k, -\frac{2lk}{n}, -\frac{2jk}{n}\right) = PPI(1, k, l, j). \quad \square$$

### 5.3. Complexity

We first compute the complexity of calculating  $\text{Res}_1$ . Each application of  $G_{k,n}$  involves the application of a 1D inverse Fourier transform followed by the computation of the fractional Fourier transform. Both the computation of the 1D inverse Fourier transform and the computation of the fractional Fourier transform require  $O(n \log n)$  operations. Thus, the computation of  $G_{k,n}$  requires  $O(n \log n)$  operations. The complexity of steps (2) and (3) in Algorithm 5.1 is of  $(3n + 1) \times n$  and  $(3n + 1) \times (n + 1)$  applications of  $G_{k,n}$ , respectively. Since each application costs  $O(n \log n)$  operations, this gives a total of  $O(n^3 \log n)$  operations for each of steps (2) and (3). The complexity of the 3D DFT in step (1) is  $O(n^3 \log n)$  and the complexity of step (4) (flipping  $T'_1$ ) is  $O(n^3)$ . This gives a total of  $O(n^3 \log n)$  for the computation of  $\text{Res}_1$ . The complexity of calculating  $\text{Res}_2$  and  $\text{Res}_3$  is identical to the complexity of calculating  $\text{Res}_1$ , and therefore the total complexity of the algorithm is  $3 \cdot O(n^3 \log n)$ , namely,  $O(n^3 \log n)$  operations.

## 6. Invertibility of the 3D discrete Radon transform

We will show that our definition of the 3D discrete Radon transform is invertible. Given the 3D discrete Radon transform  $RI$ , we show that it is possible to uniquely recover  $I$  from  $RI$ .

From Eq. (4.7)

$$R_i I = F^{-1} \circ P P_i I \quad (i = 1, 2, 3), \quad (6.1)$$

where  $F^{-1}$  (the 1D inverse Fourier transform) is invertible, and therefore left to show that  $I$  can be recovered from  $P P_i I$ ,  $i = 1, 2, 3$ .

Given the values of  $P P_i I$  (Eq. (5.2)), we take a vector of samples from  $P P_1 I$ , which corresponds to some  $k_0 \neq 0$ . From Definition 4.2,

$$P P_1 I(k_0, l, j) = \hat{I}\left(k_0, -\frac{2lk_0}{n}, -\frac{2jk_0}{n}\right) \quad l, j \in \left\{-\frac{n}{2}, \dots, \frac{n}{2}\right\}.$$

By expanding  $\hat{I}$  using Eq. (4.1) at  $(k_0, -2lk_0/n, -2jk_0/n)$ , we have

$$\begin{aligned} & \hat{I}\left(k_0, -\frac{2lk_0}{n}, -\frac{2jk_0}{n}\right) \\ &= \sum_{u=-n/2}^{n/2-1} \sum_{v=-n/2}^{n/2-1} \sum_{w=-n/2}^{n/2-1} I(u, v, w) e^{-2\pi i k_0 u/m} e^{-2\pi i (-2lk_0/n)v/m} e^{-2\pi i (-2jk_0/n)w/m}. \end{aligned} \tag{6.2}$$

Rewriting Eq. (6.2) we have

$$\begin{aligned} & \hat{I}\left(k_0, -\frac{2lk_0}{n}, -\frac{2jk_0}{n}\right) \\ &= \sum_{w=-n/2}^{n/2-1} \left( \sum_{v=-n/2}^{n/2-1} \sum_{u=-n/2}^{n/2-1} I(u, v, w) e^{-2\pi i k_0 u/m} e^{-2\pi i (-2lk_0/n)v/m} \right) e^{-2\pi i (-2jk_0/n)w/m} \\ &= \sum_{w=-n/2}^{n/2-1} c_{k_0,l}(w) e^{-2\pi i (-2jk_0/n)w/m}, \end{aligned} \tag{6.3}$$

where

$$c_{k_0,l}(w) = \sum_{v=-n/2}^{n/2-1} \sum_{u=-n/2}^{n/2-1} I(u, v, w) e^{-2\pi i k_0 u/m} e^{-2\pi i (-2lk_0/n)v/m}, \quad w \in \left\{ -\frac{n}{2}, \dots, \frac{n}{2} - 1 \right\}. \tag{6.4}$$

For fixed  $k_0, l$ , and variable  $j$  denote

$$T_{k_0,l}\left(-\frac{2jk_0}{n}\right) \triangleq \hat{I}\left(k_0, -\frac{2lk_0}{n}, -\frac{2jk_0}{n}\right).$$

Then, from Eq. (6.3) we have

$$T_{k_0,l}\left(-\frac{2jk_0}{n}\right) = \sum_{w=-n/2}^{n/2-1} c_{k_0,l}(w) e^{-2\pi i (-2jk_0/n)w/m}.$$

In other words,  $T_{k_0,l}(-2jk_0/n)$ ,  $j \in \mathbb{Z}$ ,  $-n/2 \leq j \leq n/2$ , are the values of the polynomial

$$T_{k_0,l}(x) = \sum_{w=-n/2}^{n/2-1} c_{k_0,l}(w) e^{-2\pi i x w/m}$$

at  $\{-2jk_0/n\}$ . Since we have the values of  $T_{k_0,l}(x)$  at  $n + 1$  distinct points  $\{-2jk_0/n\}$  (and thus we required  $k_0 \neq 0$ ), we can uniquely determine  $\{c_{k_0,l}(w)\}$  and  $T_{k_0,l}(x)$ , and therefore we can compute  $T_{k_0,l}(x)$  for any  $x$ .

By computing  $T_{k_0,l}(x)$  at integer points we can recover

$$T_{k_0,l}(j) = \sum_{w=-n/2}^{n/2-1} c_{k_0,l}(w) e^{-2\pi i j w/m} \tag{6.5}$$

for every  $k_0, l$ . Substituting  $c_{k_0,l}(w)$  (Eq. (6.4)) in Eq. (6.5) we obtain

$$\begin{aligned}
H_{k_0, j_0} \left( -\frac{2lk_0}{n} \right) &\triangleq T_{k_0, l}(j_0) \\
&= \sum_{w=-n/2}^{n/2-1} \left( \sum_{v=-n/2}^{n/2-1} \sum_{u=-n/2}^{n/2-1} I(u, v, w) e^{-2\pi i k_0 u/m} e^{-2\pi i (-2lk_0/n) v/m} \right) e^{-2\pi i j_0 w/m} \\
&= \sum_{v=-n/2}^{n/2-1} \left( \sum_{u=-n/2}^{n/2-1} \sum_{w=-n/2}^{n/2-1} I(u, v, w) e^{-2\pi i k_0 u/m} e^{-2\pi i j_0 w/m} \right) e^{-2\pi i (-2lk_0/n) v/m} \\
&= \sum_{v=-n/2}^{n/2-1} c'_{k_0, j_0}(v) e^{-2\pi i (-2lk_0/n) v/m}, \tag{6.6}
\end{aligned}$$

where

$$c'_{k_0, j_0}(v) = \sum_{u=-n/2}^{n/2-1} \sum_{w=-n/2}^{n/2-1} I(u, v, w) e^{-2\pi i k_0 u/m} e^{-2\pi i j_0 w/m}, \quad v \in \left\{ -\frac{n}{2}, \dots, \frac{n}{2} - 1 \right\}. \tag{6.7}$$

From Eq. (6.6)

$$H_{k_0, j_0} \left( -\frac{2lk_0}{n} \right) = \sum_{v=-n/2}^{n/2-1} c'_{k_0, j_0}(v) e^{-2\pi i (-2lk_0/n) v/m}$$

and we have that  $H_{k_0, j_0}(-2lk_0/n)$  are the samples of the trigonometric polynomial

$$H_{k_0, j_0}(x) = \sum_{v=-n/2}^{n/2-1} c'_{k_0, j_0}(v) e^{-2\pi i x v/m} \tag{6.8}$$

at  $\{-2lk_0/n\}$ . Again, since we have the values  $H_{k_0, j_0}(x)$  at  $n+1$  distinct points (for  $n+1$  distinct values of  $l$ ), we can uniquely determine  $\{c'_{k_0, j_0}(v)\}$  and the underlying trigonometric polynomial  $H_{k_0, j_0}(x)$  given by Eq. (6.8).

Evaluating  $H_{k_0, j_0}(x)$  for integer points, we obtain using Eq. (6.7)

$$\begin{aligned}
H_{k_0, j_0}(l) &= \sum_{v=-n/2}^{n/2-1} c'_{k_0, j_0}(v) e^{-2\pi i l v/m} \\
&= \sum_{v=-n/2}^{n/2-1} \sum_{u=-n/2}^{n/2-1} \sum_{w=-n/2}^{n/2-1} I(u, v, w) e^{-2\pi i k_0 u/m} e^{-2\pi i j_0 w/m} e^{-2\pi i l v/m} \\
&= \hat{I}(k_0, l, j_0). \tag{6.9}
\end{aligned}$$

Equation (6.9) states that we have recovered  $\hat{I}$  at integer grid points for every  $k_0 \neq 0$  (the entire discrete grid except the plane  $\xi_1 = 0$ ). Remains to evaluate  $\hat{I}$  on the plane  $\xi_1 = 0$ , or, in other words, the values  $\hat{I}(0, l, j)$ .

As before, by taking a sequence of samples from  $PP_2I$ , which corresponds to some  $k_0 \neq 0$ , we have from Definition 4.2

$$PP_2I(k_0, l, j) = \hat{I} \left( -\frac{2lk_0}{n}, k_0, -\frac{2jk_0}{n} \right).$$

By repeating exactly the same arguments as above we have using Eq. (4.1)

$$\begin{aligned}
 T'_{k_0,l}\left(-\frac{2jk_0}{n}\right) &\triangleq \hat{I}\left(-\frac{2lk_0}{n}, k_0, -\frac{2jk_0}{n}\right) \\
 &= \sum_{u=-n/2}^{n/2-1} \sum_{v=-n/2}^{n/2-1} \sum_{w=-n/2}^{n/2-1} I(u, v, w) e^{-2\pi i(-2lk_0/n)u/m} e^{-2\pi i k_0 v/m} e^{-2\pi i(-2jk_0/n)w/m} \\
 &= \sum_{w=-n/2}^{n/2-1} \left( \sum_{u=-n/2}^{n/2-1} \sum_{v=-n/2}^{n/2-1} I(u, v, w) e^{-2\pi i(-2lk_0/n)u/m} e^{-2\pi i k_0 v/m} \right) e^{-2\pi i(-2jk_0/n)w/m} \\
 &= \sum_{w=-n/2}^{n/2-1} c_{k_0,l}(w) e^{-2\pi i(-2jk_0/n)w/m},
 \end{aligned}$$

where

$$c_{k_0,l}(w) = \sum_{u=-n/2}^{n/2-1} \sum_{v=-n/2}^{n/2-1} I(u, v, w) e^{-2\pi i(-2lk_0/n)u/m} e^{-2\pi i k_0 v/m}, \quad w \in \left\{-\frac{n}{2}, \dots, \frac{n}{2} - 1\right\}. \quad (6.10)$$

Using  $n + 1$  distinct samples  $\{T'_{k_0,l}(-2jk_0/n)\}$  at  $n + 1$  distinct points  $\{-2jk_0/n\}$   $j = -n/2, \dots, n/2$ , we can compute  $\{c_{k_0,l}(w)\}$  and the trigonometric polynomial

$$T'_{k_0,l}(x) = \sum_{w=-n/2}^{n/2-1} c_{k_0,l}(w) e^{-2\pi i x w/m}.$$

For every  $l$  we evaluate  $T'_{k_0,l}(x)$  at integer points and by using Eq. (6.10) we obtain

$$\begin{aligned}
 H'_{k_0,j_0}\left(-\frac{2lk_0}{n}\right) &\triangleq T'_{k_0,l}(j_0) = \sum_{w=-n/2}^{n/2-1} c_{k_0,l}(w) e^{-2\pi i j_0 w/m} \\
 &= \sum_{w=-n/2}^{n/2-1} \sum_{u=-n/2}^{n/2-1} \sum_{v=-n/2}^{n/2-1} I(u, v, w) e^{-2\pi i(-2lk_0/n)u/m} e^{-2\pi i k_0 v/m} e^{-2\pi i j_0 w/m} \\
 &= \sum_{u=-n/2}^{n/2-1} \left( \sum_{v=-n/2}^{n/2-1} \sum_{w=-n/2}^{n/2-1} I(u, v, w) e^{-2\pi i k_0 v/m} e^{-2\pi i j_0 w/m} \right) e^{-2\pi i(-2lk_0/n)u/m} \\
 &= \sum_{u=-n/2}^{n/2-1} c'_{k_0,j_0}(u) e^{-2\pi i(-2lk_0/n)u/m}, \quad (6.11)
 \end{aligned}$$

where

$$c'_{k_0,j_0}(u) = \sum_{v=-n/2}^{n/2-1} \sum_{w=-n/2}^{n/2-1} I(u, v, w) e^{-2\pi i k_0 v/m} e^{-2\pi i j_0 w/m}, \quad u \in \left\{-\frac{n}{2}, \dots, \frac{n}{2} - 1\right\}. \quad (6.12)$$

Using  $n + 1$  distinct samples  $\{H'_{k_0, j_0}(-2lk_0/n)\}$  from Eq. (6.11) at  $n + 1$  distinct points ( $n + 1$  distinct values of  $l$ ),  $\{c'_{k_0, j_0}(u)\}$  is uniquely determined and

$$H'_{k_0, j_0}(x) = \sum_{u=-n/2}^{n/2-1} c'_{k_0, j_0}(u) e^{-2\pi i x u/m}.$$

Evaluating  $H'_{k_0, j_0}(x)$  at integer points and using Eq. (6.12), we obtain

$$\begin{aligned} H'_{k_0, j_0}(l) &= \sum_{u=-n/2}^{n/2-1} c'_{k_0, j_0}(u) e^{-2\pi i l u/m} \\ &= \sum_{u=-n/2}^{n/2-1} \sum_{v=-n/2}^{n/2-1} \sum_{w=-n/2}^{n/2-1} I(u, v, w) e^{-2\pi i l u/m} e^{-2\pi i k_0 v/m} e^{-2\pi i j_0 w/m} \\ &= \hat{I}(l, k_0, j_0). \end{aligned}$$

We evaluated  $\hat{I}(l, k_0, j)$  at grid points where  $k_0 \neq 0$ . Specifically, we computed  $\hat{I}(0, k_0, j)$ .

Finally, we have to compute  $\hat{I}$  on the line  $\xi_1 = 0, \xi_2 = 0$ . By using exactly the same arguments on  $PP_3I$  as above, we evaluate  $\hat{I}$  on all grid points except  $\xi_3 = 0$ . Thus, we have the values of  $\hat{I}$  on all grid points except the origin  $\hat{I}(0, 0, 0)$ . Since  $PP_1I(0, 0, 0) = \hat{I}(0, 0, 0)$  we have the values of  $\hat{I}$  on the entire grid.

Since we can recover  $\hat{I}$  (the 3D DFT of  $I$ ) from  $PP_1I$ , and trivially recover  $I$  from  $\hat{I}$ , it follows that we can recover  $I$  from  $PP_1I$ , and thus  $PP$  is invertible.

## 7. Future research

The following topics are being considered for current and future research.

**Higher dimensions:** By following the methodology employed in the construction of the 3D discrete Radon transform, we can generalize it to have Radon transforms of higher dimensions. In the construction of the 3D discrete Radon transform we employed two key paradigms that allowed generalizations into higher dimensions: (1) the representation of hyper-planes using slopes instead of normal vectors, that allows easy representation of hyper-planes at any dimension (and not just planes as in the 3D case) and (2) establishing guidelines for the selection of the transform parameters  $t$  and  $m$ . Both these paradigms can be easily extended to higher dimensions, and will be used as a basis for establishing the definition of the discrete Radon transform for higher dimensions.

Malzbender [9] and Lichtenbelt [10] showed a fast algorithm for rendering slices of a 3D discrete object using the X-ray transform and its Fourier slice theorem. Since the X-ray transform lacks a discrete definition, such algorithms involve inaccuracy from the underlying interpolation. A discrete definition for the X-ray transform that is parallel to our discrete definition of the Radon transform will enable rapid and exact Fourier volume rendering algorithms as suggested by [9] and [10].

## References

- [1] A. Averbuch, D.L. Donoho, R.R. Coifman, M. Israeli, Y. Shkolnisky, Fast slant stack: A notion of Radon transform for data in Cartesian grid which is rapidly computable, algebraically exact, geometrically faithful and invertible, *SIAM J. Sci. Comput.*, submitted for publication.
- [2] Y. Shkolnisky, A. Averbuch, R. Coifman, D. Donoho, M. Israeli, 2D Fourier based discrete Radon transform, 2002, submitted for publication.
- [3] S.R. Deans, *The Radon Transform and Some of Its Applications*, Krieger, 1993.
- [4] F. Natterer, *The Mathematics of Computerized Tomography*, Wiley, 1989.
- [5] F. Natterer, F. Wubbeling, *Mathematical Methods in Image Reconstruction*, SIAM, 2001.
- [6] A. Zygmund, *Trigonometric Series*, 2nd Edition, Cambridge Univ. Press, 1993, Vols. I, II (combined), Vol. II, Chapter X, pp. 1–6.
- [7] P.N. Swartztrauber, D.H. Bailey, The fractional Fourier transform and applications, *SIAM Rev.* 33 (3) (September 1991) 389–404.
- [8] A.K. Jain, *Fundamentals of Digital Image Processing*, Prentice–Hall, 1989, Chapter 10, pp. 431–475.
- [9] T. Malzbender, Fourier volume rendering, *ACM Trans. Graph.* 12 (3) (July 1993) 233–250.
- [10] B. Lichtenbelt, Fourier volume rendering, Technical report, Hewlett Packard Laboratories, November 1995.